University of Glasgow

Department of Electronics and Electrical Engineering

MSc. Thesis

In Fulfillment

of the requirements for the Degree

Master of Science by Research

by

Lynsey McCabe

Shaping of Spike-Timing-Dependent Plasticity curve using interneuron and calcium dynamics

June 2009

For Joan

Acknowledgements

I would firstly like to thank my supervisor Dr. Bernd Porr for allowing me the opportunity to be introduced to the field of Neuroscience as an undergraduate student, which I will always be grateful for.

I would also like to thank Maria Thompson for being a good (but fair!) critic, science colleague, and most importantly, a dear friend who has helped me many times over the past 2.5 years. A big thank goes to Laura Nicolson, Jen MacRitchie, Sam Ewing, Colin Waddell, Paolo Di Prodi and Sven Soell for their good chat and welcome distractions, such as suggestions on where to go for lunch (a vital discussion, of course) and finding out the latest updates about Bob. A massive thank you to my oldest and closest friends; Gillian Cummins, Sarahanne Doherty, Jay Dhillon, Sarah Fraser, Roisin Crumlish, Steph Coyle, Rhondda Williams, Ewen Deans, Amy Doyle and the percussion maestro, Dorothy Gunnee. You have all, in your own way, been of massive support throughout this research and beyond. I would penultimately like to give a special mention and thank you to My Friend Helen.

Finally, I would like to dedicate this to my parents Bernard and Joan McCabe whose love, support and encouragement have always been present in all that I've done throughout my life. The memory of my mum, Joan, will remain with myself, friends and family always. If I manage to be half the woman she was, with her integrity, bravery, compassion and love, then I truly will have succeeded in life.

List of Abbreviations

AMPA: α-amino-3-hydroxy-5-methyl-4-isoxezole propionate.

AMPA-R: α-amino-3-hydroxy-5-methyl-4-isoxezole propionate receptor.

AP: Action Potential.

BPAP: Back-Propagating Action Potential.

Ca^{2+}**:** Calcium ion.

$[Ca^{2+}]_i$**:** Intracellular Calcium concentration.

Cl^{-}**:** Chloride ion.

DNA: Deoxyribonucleic acid.

EPSC: Excitatory Postsynaptic Current.

EPSP: Excitatory Postsynaptic Potential.

GABA: γ-amino-butyric acid.

GABA-R: γ-amino-butyric acid receptor.

HFS: High-Frequency Stimulation.

IPSC: Inhibitory Postsynaptic Current.

IPSP: Inhibitory Postsynaptic Potential.

K^{+}**:** Potassium ion.

LTD: Long Term Depression.

LTP: Long Term Potentiation.

Na^{+}**:** Sodium ion.

NMDA: N-Methyl-D-aspartic acid.

NMDA-R: N-Methyl-D-aspartic acid receptor.

Mg^{+}**:** Magnesium ion.

STDP: Spike-Timing-Dependent Plasticity.

Abstract

The field of Computational Neuroscience is where neuroscience and computational modelling merge together. It is an ever-emerging area of research where the level of biological modelling can range from small-scale cellular models, to the larger network scale models. This MSc Thesis will detail the research carried out when looking at a small network of two neurons. These neurons have been modelled with a high level of detail, with the intention of using it to study the phenomenon of Spike-Timing-Dependent Plasticity (or STDP). Spike-Timing-Dependent Plasticity is the occurrence of either a strengthening or weakening in connection between two neurons, depending on the temporal order of stimulation between them. A major part of the work detailed is the focus on what mechanisms are responsible for these changes in plasticity, with the goal of representing the mechanisms in a single learning rule. The results found can be directly compared to data previously seen by scientists who worked on in-vitro experiments. The research then goes on to look at further applications of the model, in particular, looking at certain deficits seen in people with Schizophrenia. We modify the model to include these cellular impairments, then observe how this affects the standard STDP curve and thus affects the strengthening/weakening between the two neurons.

Contents

1 Introduction

Computational Neuroscience is a field which has developed exponentially within the past twenty years. Throughout the past decade it has also become an area which has received serious credibility and collaboration from the neuroscience community. A large part of its fruition is due to the increase in processing power that computers now have, allowing for more finer detailed models and simulations to be realised, while reducing the run-time required to simulate them. With the extra power and speed available, computational neuroscientists have a greater freedom when creating neuron or brain models from the detailed cellular level to the larger-scale network-level. Examples of network-level models are the scientists who have studied the visual cortex, with very successful results in replicating these processes [1, 2].

There has been a lot of focus on computational neuroscientists working alongside biologists in creating realistic cell and network models, in the hope of testing/hypothesising theories or producing potential pharmacological cures for neurological disorders.

One of the first types of realistic neuron models was developed by scientist Wilfrid Rall, who used "Cable Theory" to come up with a multicompartmental model of the neuron with dendrites and axon [3, 4, 5, 6]. In more recent times, a high-profile project underway is the "Blue Brain project" [7] managed under the collaboration of IBM and the Ecole Polytechnique Federale de Lausanne, who, using the Blue Gene supercomputer, are currently modelling a biophysically realistic cortical column.

1.1 Research Focus

The research focus over the past two years has centered on the study of synaptic plasticity in a microcircuit of two neurons. A brief definition of plasticity is to characterise it as the strength in connection between the two synaptic terminals (end points) of a neuron. This definition of plasticity will be further elaborated on in Section 7. The microcircuit consists of a pyramidal neuron with attached interneuron. Put simply, this circuit consists of an excitatory (pyramidal) cell innverating

a smaller (interneuron) cell which in turn performs a negative feedback, or inhibition, onto the excitatory cell. The pyramidal neuron simply gets its name from its cell body (also known as the soma) resembling the shape of a pyramid. Interneurons are a type of smaller neuron that project onto larger neurons like pyramidal cells and are generally inhibitory in nature, by reducing the "excitatory" activity of these pyramidal neurons. What is the reason for looking at a circuit of two neurons? Looking at the ability to make neural connections in these microcircuits (also known as plasticity) is of great interest, in particular when comparing these results with similar experiments carried out in-vivo and in-vitro.

1.2 Abstraction level of model

One main objective is to take this small network of two neurons, add the detail of ionic channels and certain receptors which interact during cell firing, then develop theories on how these mechanisms actually work during processes such as learning. Thus, the research is not focused on the brain's higher-level behaviourism of learning itself, but instead, it is focused around the *level of detail* required or comprised in developing the cellular model of the neuron, in particular hypothesising which cellular mechanisms play key roles in synaptic plasticity, the phenomenon associated with memory and learning.

There are two other major considerations which have to be evaluated before a model can be constructed, and both are of equal importance. The first is deciding what exactly should be modelled and what can safely be ignored. To do this, we have to look at the physiology of the neuron and observe how these properties/characteristics should be expressed computationally. The second, which will be discussed in more detail in consequent chapters, is what approach to computational modelling is most suitable for the research, i.e is it a viable option to use a software package such as the GENESIS [8] package used for this research?

1.3 GENESIS - What is it?

For this research, the software package “GENESIS” [8] was decided on as suitable to model the cortical microcircuit. GENESIS is an open-source software package, with its acronym standing for GEneral NEural SImulation System. The developers state that it is a: “General purpose simulation platform developed to support simulation of neural systems ranging from subcellular components and biochemical reactions to complex models of single neurons, simulations of large networks, and systems-level models”. The GENESIS programming language is similar to C and allows modification of the software if required for more complex models. If the user wishes to add code to the simulator, this can be done in C. Recompiling of the source code allows the new functions to then become part of the GENESIS structure. For the purpose of research demands, we have written a new object which satisfactorily implements learning processes. Fragments of this code will be shown in later sections. The software’s hierarchical structure will also be discussed in the following sections. Before any of the programming decisions can be discussed, we have to firstly look at the physiology of the neuron to get a better understanding about how neurons behave.

2 Physiology of the Neuron

To be capable of sufficiently modelling the neuron, we look at its physiology, and in particular, the characteristics of the neuronal membrane. In mammals, the central nervous system (CNS) consists of the brain and spinal cord and there are approximately 10 billion neurons present. Each cell then connects through to tens of thousands of other cells. On the next page is a diagram of a typical neuron which can be found in the central nervous system. It is appropriate to note that interneurons are similar to the figure below, but stereotypically have short or no axon part to them and are generally inhibitory by nature.

A typical neuron, as seen in Fig. 1, consists of a soma, axon (and axon hillock which joins the soma to the axon), neuronal membrane separating the outside of the cell from the inside and dendrites which transmit signals to nearby neurons. The soma is also known as the *cell body* and

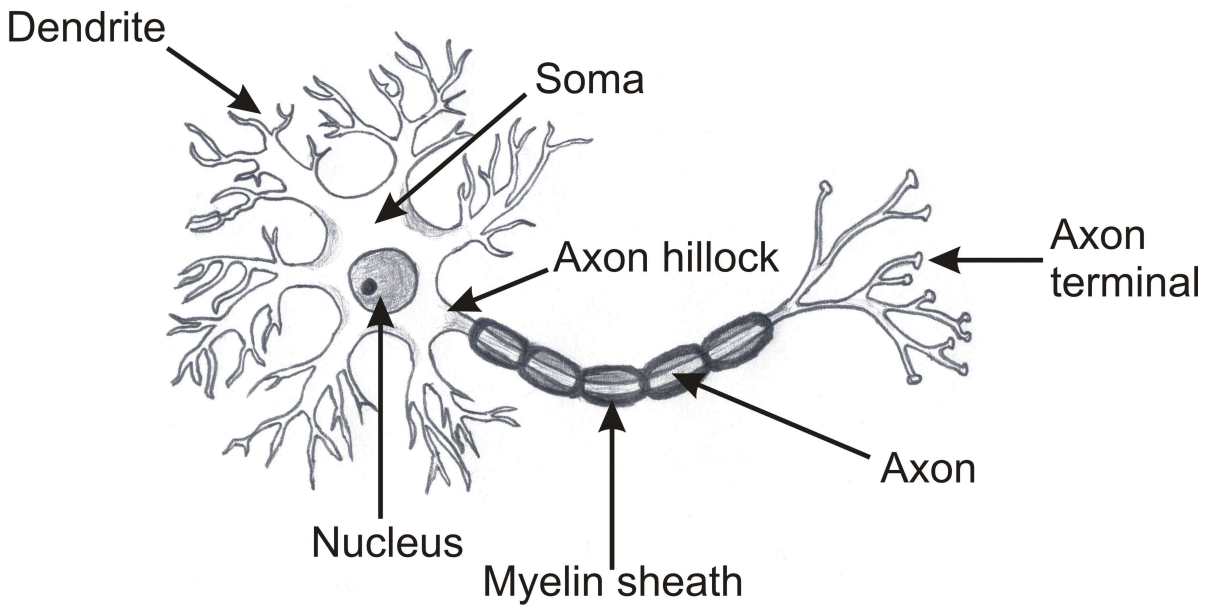

Figure 1: Sketch of typical neuron. The neuron is made up of the soma (or cell body), axon and dendrites. The neuron has a membrane which separates the fluid inside the cell from the outside. The dendrites are branch-like and are the point (in many neurons) where electrical signals are transmitted to. This signal is propagated down the neuronal body towards the axon, which then transmits across the cell to the next dendrite.

is generally spherical in shape. Inside the soma is a fluid called cytosol; the clear internal fluid of the cell containing proteins necessary for synaptic transmission amongst other important roles. Inside the soma is the cell-nucleus which is made up of DNA molecules and proteins. The axon part of the neuron is where signals are transmitted from the cell body, down through the axon from the “terminal button” and across the “synaptic cleft” - the space between the presynaptic neuron and postsynaptic neuron. The axon itself is covered by a myelin sheath, which acts as an insulator to the axon, keeping the electrical impulses generated from the cell body from travelling outward before reaching the axon terminal and across to the dendrite of another neuron. Dendrites are branch-like in nature and are where the presynaptic signals are transmitted to, with some of the

transmitters being sent back to the presynapse (a phenomenon known as “re-uptake”). This is of course a simplified explanation of what happens during synaptic transmission, and this process will be further clarified later in the report.

2.1 The “Passive” neuronal membrane

The passive membrane of a neuron separates the inside of the cell from the outside. When we look at circuit equivalents, we will see it can be successfully represented by a simple RC circuit.

Firstly, it is important to look at the components which the membrane is physiologically made from, then express its electrical properties in a simple circuit format. This allows a clearer approach to be used when constructing a circuit equivalent model of the cells. The *phospholipid bilayer* is what the cell membrane is primarily composed of. It consists of a layer of lipid molecules made up from polar heads and non-polar fatty-acid tails. These tails face each other with the polar heads pointing outwards, thus meaning the bilayer is able to separate the intracellular and extracellular fluid.

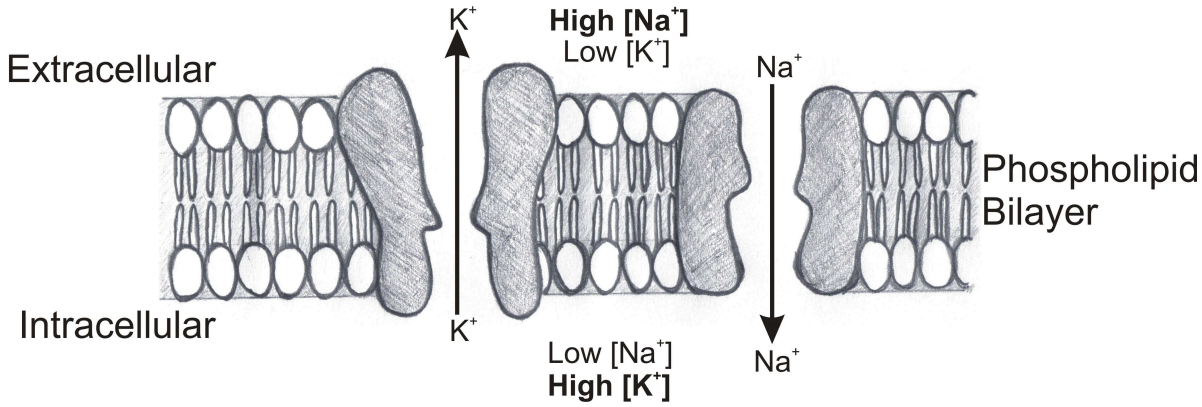

Figure 2: Phospoholipid Bilayer. The phospholipid bilayer is how the neuronal membrane separates the intracellular fluid from the extracellular. Inserted into the membrane are proteins known as ion-channels which, when open, can allow the influx and outflux of ions such as potassium and sodium.

Inserted into the lipid bilayer are proteins known as ionic-channels and receptors. These allow ions such as sodium and potassium to flow in and out of the membrane using gate-like mechanisms. When the cell is at rest, the sodium and potassium ions inside the cell (intracellularly) sit at a ratio

of a low concentration of Na^+ ions to a high concentration of K^+ ions. Outside the cell, or extracellularly, there is a low concentration of potassium ions in comparison to a higher concentration of sodium (Na^+).

The phospholipid bilayer acts as a membrane capacitance, and in fact has a very high capacitance due to being almost impermeable to ions. This is with the exception of those ions moving through gated channels under certain "permissive" conditions. The membrane capacitance, C_m, is the measurement of how much charge has to be spread across the membrane for a voltage potential, V_m, to build up ($Q = CV_m$).

When the potential difference between the extracellular voltage changes with respect to the intracellular voltage, a current will begin to flow across the capacitance, I_c. This is calculated by differentiating $Q = CV_m$ and is as follows:

$$I_c = C\frac{dV_m(t)}{dt} \tag{1}$$

As mentioned, a passive membrane can be represented by an RC circuit (Figure 3). This is true if assuming the neuron is of a small spherical space with diameter "d" and the total membrane area given by πd^2[9]. The total capacitance C is given by multiplying the membrane capacitance C_m by the membrane area. The current through the resistance I_R is given by subtracting the resting voltage potential from the membrane potential and dividing by R:

$$I_R = \frac{V_m - V_{rest}}{R} \tag{2}$$

When applying a fixed current such as the current injection, the membrane capacitance C_m forces a limit on how quickly the membrane potential V_m can change. Thus for larger membrane capacitances, a slower change in membrane voltage is seen. During this passive state, it is important to note that there is no charge moving across the intracellular membrane. As the membrane voltage changes, a change in charge occurs allowing current to flow, represented by Eq. 1. The current itself never flows across the capacitance and the charge is distributed across both sides of the membrane.

The extremely high resistivity of the lipid bilayer means that it prevents any large amounts of charge from passing across the cell membrane. This membrane resistivity is roughly around one billion times higher than that of the intracellular fluid, cytoplasm. In terms of the circuit discussed so far, this means the membrane can be adequately represented by the capacitance, C_m.

Proteins which are embedded in the cell membrane act as "gates" in the phospholipid bilayer. These gates allow ions to pass in and out of the membrane in addition to allowing the transmission of information/signals. The proteins can be ion channels, neurotransmitters, receptors, pumps and enzymes. For the purpose of this research, we only focus on ion channels (also known as pores) and certain receptors which are integral in synaptic plasticity.

For further simplicity, we describe the flow of current through the ionic channels by using a simple linear resistance, R (Eq. 2). As we also have to consider the membrane resting potential, we have a simple circuit that consists of C, R and V_{rest} which describes the "passive" behaviour of the membrane. This membrane resistance is usually known as the "specific membrane resistance", R_m, and has units $\Omega\cdot$ cm^2. The resistance (R) can be calculated by dividing R_m by the membrane area in question. The passive conductance per unit area of membrane is known as the "specific leak conductance", $G_l = \frac{1}{R_m}$, and has units $S/$ cm^2. We can look at these components briefly in a simple RC circuit (Fig. 3).

If initial conditions are applied to Eq.1, then the voltage trajectory can be modelled. By assuming that the membrane potential at time t = 0 is equal to the resting potential when there is no input (I_{inj} = 0, V_m(t = 0) = V_{rest}), we can say that $\frac{dV_m}{dt} = 0$. This means that when the cell is at rest and is receiving no input from a current pulse, the cell will continue to remain at V_{rest}.

Applying a step current $I_0 = I_R + I_C$ with constant amplitude at t = 0, Eq.1 can then be rewritten as:

$$V_m(t) = v_0 e^{\frac{-t}{\tau}} + v_1 \tag{3}$$

where v_0 and v_1 depend on the initial conditions. Applying a current allows the voltage to change *just* enough to cause a potential difference across the membrane, without causing it to surpass the

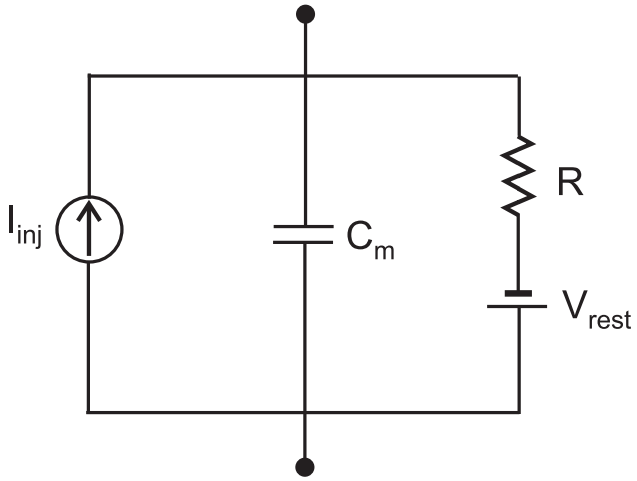

Figure 3: Simplified circuit diagram of the passive neuronal membrane. The capacitance, C, represents the high membrane resistance from the phospholpid bilayer, with the parallel resistance R being the passive membrane resistance, V_{rest} the resting membrane potential, and I_{inj} the input into the circuit.

"threshold voltage", where spiking would occur.

By substituting Eq. 3 into Eq. 1 and cancelling out any duplicate variables yields:

$$v_1 = V_{rest} + RI_0 \tag{4}$$

We can find v_0 by applying the initial condition $V_m(t = 0) = v_0 + v_1 = V_{rest}$. V_m can then be calculated by setting the steady-state voltage potential of the cell in response to the current when $V_\infty = RI_0$:

$$V_m(t) = V_\infty(1 - e^{\frac{-t}{\tau}}) + V_{rest} \tag{5}$$

This means that the membrane potential V_m deviates away from V_{rest} at an exponential rate, with time constant τ. How quickly it actually diverges depends on the time constant $\tau = RC$. Thus, the smaller or larger the capacitance, then the smaller or larger the current required to charge it, respectively.

It has been mentioned that a constant current source can be used as an excitatory input to the neuron to allow changes in the behaviour of the membrane voltage. When observing real neurons,

it is seen that inputs into the neuron come from excitation or inhibition of the membrane voltage through receptors and ion channels embedded on the cell membrane. The next section describes some inputs to the cell which cause this rise or decline in membrane potential.

3 Synaptic input into a neuron

For any activity to be initiated in a neuron, there has to firstly be some input to the presynaptic side of the cell to invoke either an excitatory response (rise in membrane voltage), or inhibitory response (fall in membrane voltage) in the postsynaptic neuron.

The communication of neurons through "point-to-point" contact, when the end points (or *terminals*) meet, is known as *synaptic transmission*.

A typical synaptic connection is made up from the connection between a presynaptic terminal (usually the axon terminal) and a postsynaptic terminal located either on the dendrite, or cell body (soma), however, there are occasions where the contact is via dendrite-dendrite or axon-axon connections.

3.1 Characteristics of synaptic transmission

The characteristics of synaptic transmission can be split into three stages between the presynaptic terminal and postsynaptic neuron, as seen in Fig.4.

The process of synaptic transmission is started when an action potential travels down the axon to the presynaptic terminal. At this point, calcium ions flow into the presynapse. This causes "vesicles" (stores of neurotransmitters) to move downwards and fuse to the membrane where the neurotransmitters are released. The neurotransmitters travel across the gap separating the pre- and postsynaptic membrane called the "synaptic cleft". The neurotransmitters then diffuse across this cleft (travelling from a higher concentration level to a lower) and bind to the receptors on the postsynapse. For example, these neurotransmitters could bind to sodium channels and allow an influx of sodium to the postsynaptic cell. As sodium ions are positively charged, the associated positive

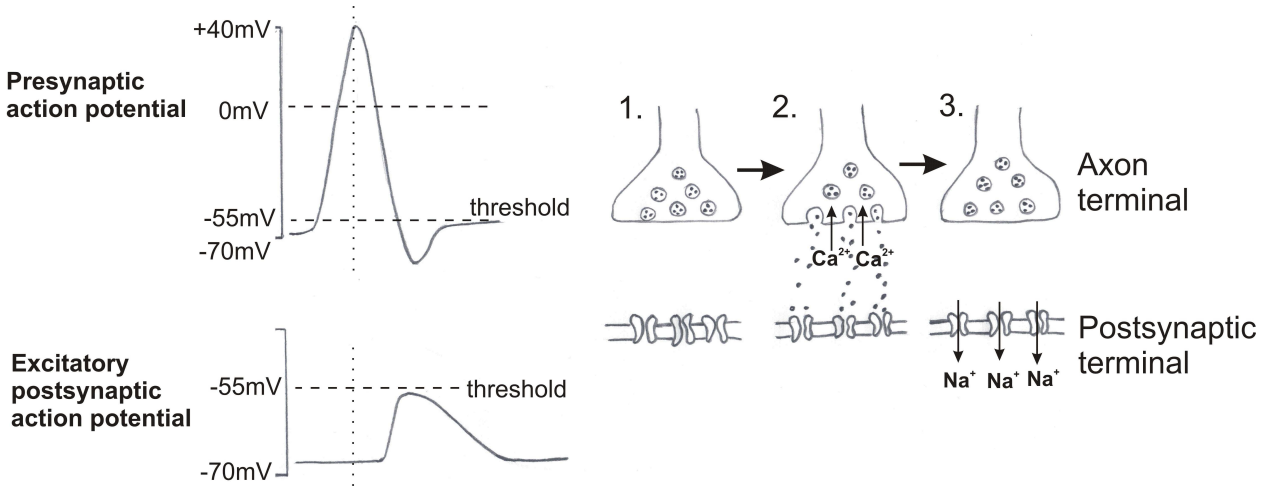

Figure 4: Diagram of Stages in Synaptic Transmission. Diagram is redrawn from Jessel and Kandel's paper on synaptic transmission[10]. (1). The action potential propagates from the soma to the axon terminal. (2). Calcium channels on the axon terminal open to allow Ca^{2+} ions to flow inwards and fuse to the membrane, causing neurotrasmitters to be released across to the postsynaptic neuron. (3). These neurotransmitters bind to the postsynaptic neuron, causing ion channels to open and Na^{+} ions to flow into the cell.

current carried by the ions (known as an excitatory postsynaptic current, or, EPSC) would lead to a rise in the membrane potential for around 1ms known as an excitatory postsynaptic potential (EPSP).

The interaction between different neurotransmitters and receptors on the postsynaptic terminal causes many diverse actions in synaptic transmission such as "fast synaptic transmission". Fast synaptic transmission is the quick onset of associated excitatory or inhibitory postsynaptic currents, usually occurring at times $<$1 ms, with their durations lasting less than 20 ms.

The majority of "fast synaptic transmission" is governed by amino acids. These acids can be split into those which are excitatory in nature (causing or adding to the generation of an action potential), and those which are inhibitory decrease the possibility of an action potential to be elicited. The main excitatory neurotransmitters which bind to postsynaptic receptors are known as *glutamate* and *aspartate* and the inhibitory neurotransmitters are γ-amino-butyric acid (GABA) and *glycine*.

3.1.1 Receiving Input - Postynaptic Receptors

Postsynaptic receptors can be split into two different types. The first are those which are directly coupled with ion channels, known as "ionotropic receptors". Binding of a neurotransmitter to an ionotropic receptor leads to the fast opening of the linked ion channels. Examples of these ionotropic receptors are the $GABA_A$ receptor, the NMDA receptor (N-Methyl-D-aspartic acid) and non-NMDA receptors such as AMPA (α-amino-3-hydroxy-5-methyl-4-isoxezole propionate) receptors. All of these receptors will be further elaborated on throughout this section. The second type of receptor is known as a "metabotropic receptor". With the metabotropic receptor, binding of a neurotransmitter activates a "second messenger" such as calcium ions. Once the second messenger diffuses to its destined site "of action", it binds to a particular ion channel to modulate the properties of the channel. The special properties of calcium will also be furthered upon in later sections.

3.2 Excitatory and Inhibitory Currents

Activation of a synapse that is excitatory results in a synaptic current I_{syn} which depolarises the postsynaptic membrane. This current causes a momentary rise in membrane potential known as an EPSP. However, activation of an inhibitory synapse can either cause the membrane potential to remain around the membrane potential V_{rest}, or cause an *outward* current to flow. This outward current would produce a momentary dip in voltage that hyperpolarises the cell. This dip is known as an inhibitory postsynaptic potential, or IPSP. Put simply, activation of an excitatory synapse results in a positive current injection *into* the cell, whereas activation of an inhibitory synapse allows the outward flow of current from the cell, causing an IPSP.

3.3 Excitatory Synaptic Input

The majority of fast excitatory neurotransmitters found in the central nervous system of vertebrates are glutamate. The application of glutamate or aspartate on neurons causes fast depolarisation of

the postsynaptic cell. There are two distinct classes of excitatory glutamate synapses known as NMDA and non-NMDA synapses. Those non-NMDA synapses bind to agonists such as AMPA. The other glutamate receptor called an NMDA receptor, reacts differently from the former as will be explained shortly. What now will be described is the process undergone when an action potential travels down towards the presynaptic terminal releasing glutamate across the synaptic cleft toward a postsynaptic AMPA receptor.

3.3.1 AMPA Receptor

During an action potential, the excitatory amino-acid, glutamate, is released from the presynaptic terminal. When the glutamate has diffused across the synaptic cleft and bound to the postsynaptic AMPA receptor, its associated channel opens, allowing sodium and potassium to flow across the membrane. At non-NMDA receptors such as ionotropic AMPA receptors, the postsynaptic channels activate very quickly. The peak value of the synaptic current usually occurs very quickly ($<$ 1ms) with an exponential decay with time constant ranging between 0.5 ms and 3 msec. Wilfrid Rall described the time course of the synaptic conductance of the AMPA receptor as an alpha function [11]. This alpha function is used to describe a "smooth" conductance change, rather than some approximations which use a rectangular pulse. It is also used in the GENESIS software (discussed in later sections) and is described as follows:

$$g_{syn}(t) = g_{max}\frac{t}{t_p}e^{(1-t/t_p)} \tag{6}$$

The function increases transiently to a maximum conductance g_{max} at $t = t_p$. After the function peaks at its maximum, the conductance $g_{syn}(t)$ has a slow decline back to zero. Fig.5 shows the smooth conductance change seen when ions pass through AMPA receptors compared to the slower conductance change though NMDA receptors.

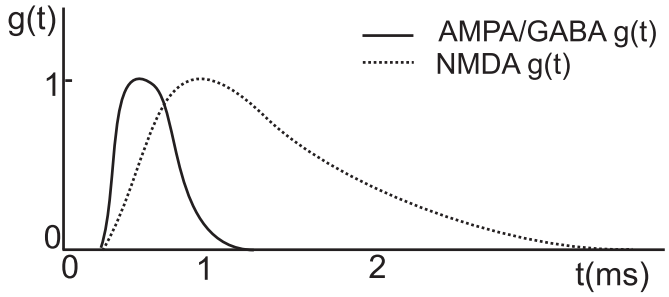

Figure 5: Conductance change comparison between AMPA/GABA receptors and NMDA-receptors. The single alpha function characterises the fast synaptic conductance change from the AMPA receptors, whereas the NMDA receptor has a slower rise and decay time described by a dual-alpha exponential function.

3.3.2 NMDA Receptor

Unlike the non-NMDA receptor, the conductance change associated with the NMDA receptor is dependent on the membrane potential voltage, V_m.

If the cell membrane of the postsynaptic neuron is at rest when glutamate is bound to the NMDA receptor, the receptor opens, but is also blocked by magnesium ions which sit in front of the NMDA receptor. As the postsynaptic membrane becomes depolarised, the magnesium ions move outward from the receptor and the NMDA receptor becomes permeable to sodium, potassium and calcium ions, as visualised in Fig.6.

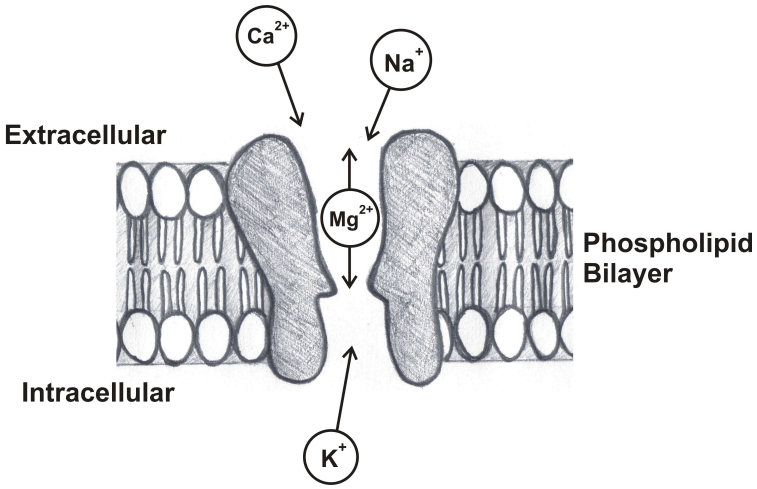

Figure 6: Ions travelling through NMDA-receptor once magnesium block is lifted.

The NMDA conductance has a significantly slower time-course in comparison to the AMPA conductance. This is a result of the receptor's dependence on the cell membrane potential, V_m,

as well as being dependent on magnesium, which obstructs the NMDA-R until the cell becomes depolarised. This then allows the receptor to become permeable to Na^+, K^+ and Ca^{2+} ions.

The voltage-dependent NMDA conductance, $g_{NMDA}(t)$, is calculated from the following [9]:

$$g_{NMDA}(t) = \bar{g}\frac{e^{\frac{-t}{\tau_1}} - e^{\frac{-t}{\tau_2}}}{1 + \eta[Mg^{2+}]e^{-\gamma V_m}} \tag{7}$$

With rise and decay times τ_1 = 2 ms, τ_2 = 100 ms and maximal conductance, $\bar{g}$. The Magnesium-block parameters are: γ = 0.06/mV, η = 0.33/mM and magnesium concentration, $[Mg^{2+}]$ = 2mM.

This voltage-dependent conductance, $g_{NMDA}(t)$, increases as the cell is depolarised.

These are the main excitatory receptors which are used in the microcircuit model for the research undertaken. We now look at inhibitory receptors, in particular GABA receptors, which are responsible for causing inhibition, and sometimes under special circumstances, cause excitation.

3.4 Inhibitory Synaptic Input - GABA Receptors

GABA receptors are usually located in the membrane of excitatory neurons and receive innervation from inhibitory neurons such as interneurons. There are two types of postsynaptic receptors associated with GABA-releasing terminals, called $GABA_A$ and $GABA_B$ receptors. Both act differently from each other, with the common factor being that both bind GABA. For the purpose of this report and model to date, we only look at the $GABA_A$ receptor. Like the AMPA receptor, the $GABA_A$ receptor is *ionotropic*. The result of GABA binding to the receptor is the opening of chloride channels. Chloride ions are generally present inside and outside of the cell, with the majority concentrated on the outside. When the chloride channels open, a flow of negatively charged chloride ions move into the cell causing a change in conductance to be seen. The change in postsynaptic conductance from the influx of the negatively charged ions rises very rapidly ($<$1ms), and decays within 10-20ms. Thus, the conductance change can be approximated again by Rall's single-pool alpha exponential model.

A characteristic which separates the $GABA_A$ receptor from its excitatory NMDA and non-

NMDA counterparts is that the location of the $GABA_A$ receptor can be found on the soma of the neuron, as opposed to the dendrite or axon.

It was found by Aihara [12] and also discussed by Edward O' Mann [13] that fast GABAergic transmission onto other cells can cause a phenomenon known as "shunting inhibition" [13]. GABA receptors are connected to chloride channels (Cl^-) which have a reversal potential near to that of the resting membrane potential of the pyramidal cell ($E_{Cl^-} \approx E_{rest} \approx -65mV$). When the Cl^- channels are activated they cause brief, but significant, changes to the membrane potential, V_m resulting in large increases in conductances leading on to the generation of an inhibitory postsynaptic potential. This is the process of shunting inhibition. This shunting inhibition is of great interest, particularly when observing what effect this inhibition has on plasticity in the small microcircuit model.

Now we have an idea of what types of receptors allow synaptic input to the neuron, we can then look at what happens when there is repeated stimulation to the inputs of a neuron, which result in the generation of action potentials and begin the process of synaptic transmission leading to plasticity changes.

4 The Action Potential

In neurophysiology, an action potential is also known as a "nerve impulse", or "spike", and is usually one or more short voltage pulses which propagate downwards from a cell's membrane. They are also generated in the nerve fibres of cells controlling muscular function, but we are only interested in action potentials generated from the neuron cell-body and travel down the axon. When a cell is at rest, the voltage inside is negative and sits approximately between -65mV and -70mV depending on the type of cell. The action potential can be thought of as a brief reversal of the resting membrane potential when the inside of the cell becomes positively charged. This is known as *depolarisation*.

Figure 7 shows how a generalised action potential looks, but these can vary slightly in different

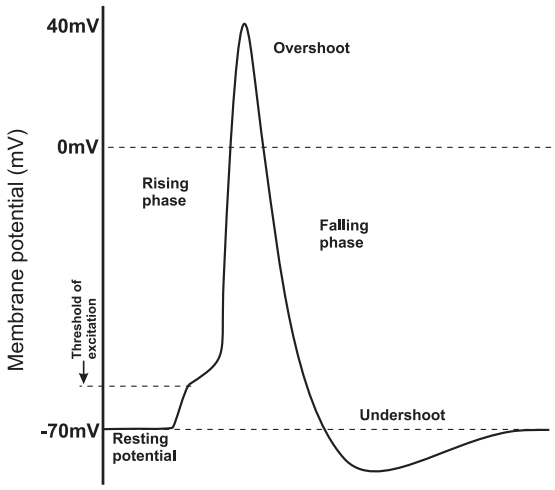

Figure 7: Diagram of Stages in Action Potential generation. (1). Once the threshold of excitation has been reached (-65mV), sodium channels open allowing the positively charged Na^+ ions to enter. At the same time, potassium channels open, allowing the negatively charged K^+ ions to leave the cell, driving the membrane potential close to the equilibrium potential for N^+ ions. (2). After 1ms when the voltage is at its peak, the Na^+ channels begin to close. Potassium ions leave the cell and the membrane voltage is driven down towards the equilibrium potential for K^+ ions. (3). As the membrane potential is driven down towards the resting potential, it undershoots towards the K^+ equilibrium potential. The potassium channels close and any excess potassium is diffused away.

cell types in vertebrates and invertebrates. The first part of the action potential is known as the "rising phase" and is characterised by a quick, steep depolarisation of the cell membrane until it reaches around +40mV (equilibrium potential for sodium). The next stage of the action potential, where the voltage rises above 0V and rushes towards +40mV, is known as the "overshoot". After this we have a repolarisation of the cell as it is driven back negatively towards the resting potential for potassium ($\approx$ -80mV), and actually becomes more negative than the cell resting potential itself. This part of the action potential is known as the "falling phase". As the potential is driven to a value more negative than the resting potential, it is known as the "after-hyperpolarisation" or "undershoot" for short. Due to a process from the "sodium-potassium" pump the balance of sodium/potassium ions is restored intracellularly and extracellularly, by the exchange of 3 sodium ions inwards for every 2 outwards. This allows the membrane potential to return to its resting potential of $\approx$ -65 millivolts. Usually this process lasts around 2 ms, and during this hyperpolarisation there is a period known as the "absolute refractory period", where it is physically impossible for another action potential to

be invoked due to the sodium channels remaining in an inactive state. When we go on to look at the more detailed Hodgkin and Huxley model, the ionic processes of the action potential will be explained in more detail.

Firstly, we begin by implementing a simple spiking (the invocation of action potentials) model for which we can add in realistic synaptic inputs and ionic processes to. We will use a "leaky integrate and fire" model. Viewed as a simplistic model by many, it was recently investigated by Jolivet et al [14] that in fact the integrate and fire model was highly accurate in modelling spike trains seen in real neurons.

5 The Leaky Integrate and Fire model

The integrate and fire model originates from Stein and others [15, 16], basing their work on a spiking cell model by Lapicque at the beginning of the twentieth century [17, 18]. The reason for its popularity is that it manages to successfully represent two important characteristics of the spiking neuron. The first is the integrating nature of the passive, subthreshold "domain" when the cell is resting, which integrates any excitatory or inhibitory inputs to the cell. The second property is the models ability to produce spiking once the threshold voltage has been reached. The integrate and fire model's can come in many varieties, with the most well known being the "*perfect* integrate and fire model" and the "*leaky* integrate and fire model".

The perfect integrate and fire model can be represented by a sole capacitor, which integrates any charge received by synaptic inputs with a set voltage threshold for spiking. Opposed to the perfect model is the leaky integrate and fire model, which has the addition of a resistance, R, to include any leakage currents through the cell membrane. It also models the decay of the membrane potential after spiking effectively.

If using a simple, sole, capacitor, then any input current the circuit receives will be summated linearly:

$$C\frac{dV(t)}{dt} = I(t) \tag{8}$$

Equation 8 determines the subthreshold time course for the cell's membrane potential, if initial conditions are applied. When the membrane potential reaches threshold, V_{th}, a spike is initiated and the charge built up on the capacitance is "shunted" back to zero by a switch. In the cell membrane this is done by various ionic conductances flowing inwards and outwards of the cell, which shall be discussed in the Hodgkin-Huxley model section. It can be seen from this equation that the firing rate is linearly related to the input current, as the output is based on the integration of the input current, $I(t)$.

However, when referring back to Section 2 detailing the passive neuronal membrane, the leaky integrate and fire model (Fig. 8) allows for a more realistic behaviour by introducing the *leak resistance* R. The leak resistance being the conductance/resistance resulting from ions flowing in

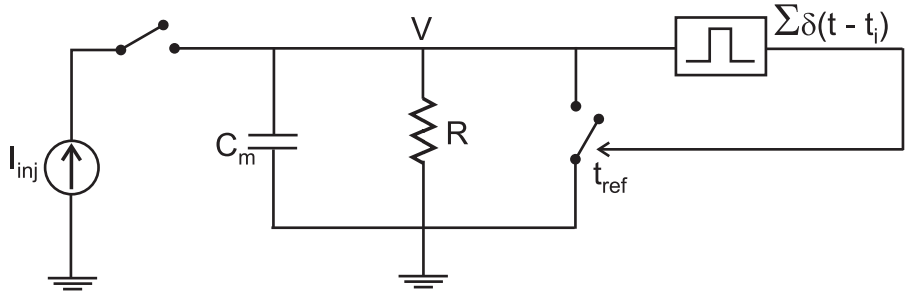

Figure 8: Diagram of Leaky-Integrate and Fire circuit.

and out the membrane during the cell's resting potential. Rewriting Eq.8 with the inclusion of the leak resistance is then:

$$C\frac{dV(t)}{dt} + \frac{V(t)}{R} = I(t) \tag{9}$$

If we multiply this equation by R then we can introduce the membrane time constant $\tau_m = RC$. We then get:

$$\tau_m\frac{dV(t)}{dt} = -V(t) + RI(t) \tag{10}$$

We know from the previous section that the subthreshold voltage is dependent on the input current, $I(t)$, with respect to the time constant $\tau = RC$ (Equation 5). The time frame of the membrane potential responding to a step of constant current, remaining on from time t=0, is solved below by setting t to zero:

$$V(t) = IR(1 - e^{\frac{-t}{\tau}}) + V(t = 0)e^{\frac{-t}{\tau}} \tag{11}$$

The membrane potential then charges upwards at an exponential rate to its stationary maximum value $V = IR$. Looking at Fig.9, we can see the membrane voltage in response to a current injection.

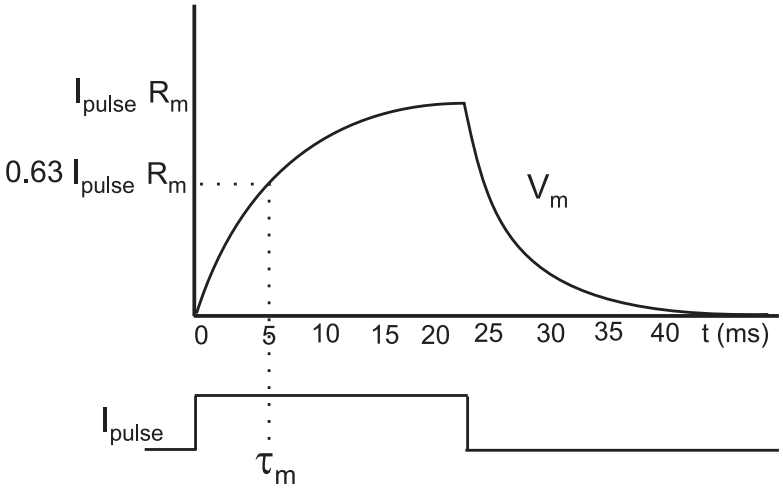

Figure 9: Voltage response to current pulse. Voltage increases until it reaches its maximum, $I_{pulse}R_m$.

The leaky integrator model will only remain true to Eq.11 for voltage values beneath the threshold, V_{th}. This is due to the voltage being reset to zero once the threshold for reaching spiking has been met.

The threshold current required for an action potential is:

$$I_{th} = \frac{V_{th}}{R} \tag{12}$$

For any current, I, which passes the threshold I_{th}, an output impulse will be generated at time

T_{th}, such that $IR(1 - e^{\frac{-T_{th}}{\tau}}) = V_{th}$ remains true. By rearranging this to solve for T_{th}, the time to see a voltage spike can be calculated as:

$$T_{th} = -\tau ln(1 - \frac{V_{th}}{IR}) \tag{13}$$

If we presume that the current input is still present when the voltage is reset after an impulse, the membrane will once again charge towards the membrane threshold and trigger another spike at time $T_{th} + t_{ref}$. t_{ref} is known as the refractory period, and is the time taken between the voltage resetting to zero and restarting the process of charging. This is shown diagrammatically in Fig.10.

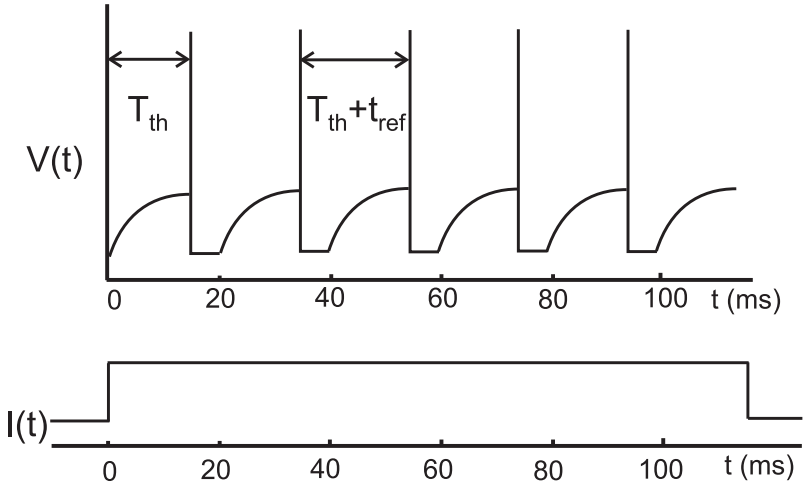

Figure 10: Spiking of LIF circuit during current pulse. The membrane voltage charges towards its membrane threshold which evokes another spike at time $T_{th} + t_{ref}$. The time taken between the voltage dropping back to zero and charging again is known as the refractory period, t_{ref}.

Now that we have an idea of how, theoretically, spiking neurons can be modelled, we progress to looking at which biological processes take place for the generation of spikes. By introducing the Hodgkin and Huxley parameters to the model, we can then incorporate the influx and outflux of ions which determine the membrane voltage once a current injection has been applied.

6 Hodgkin and Huxley model

Hodgkin and Huxley are well-known names in the field of neuroscience due to their groundbreaking work to describe ionic processes and voltage dependent conductances during an action potential, which they studied on a giant squid axon [19, 20, 21, 22]. These studies lay the foundations of many modelling techniques such as compartmental modelling [23]. However, as we will discover further on, only describing the potassium and sodium conductances is not sufficient for the depth of detail required for the model, and other conductances have to be taken into consideration. Part of Hodgkin and Huxley's work was to formulate equations allowing the mathematical description of ionic processes seen during an action potential. To understand what this exactly means, it is now necessary to look at the action potential more in-depth to observe what takes place inside and outside the cell membrane.

6.0.1 Generation of The Action Potential - In the Cell

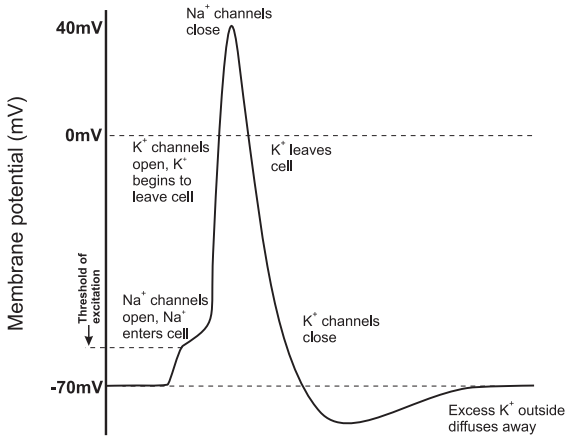

Figure 11: Diagram of invoked action potential. When the membrane receives stimulation from an excitatory input, the membrane voltage has a brief rise in the positive direction. If the membrane continues to receive stimulation to push the voltage above the "membrane threshold", sodium channels open and an action potential is elicited. The voltage is driven upwards towards the equilibrium potential for sodium ions (+62 mV). After 1ms, the sodium channels close and the cell voltage is driven downwards towards the equilibrium potential of potassium ions (-80 mV). Also at this point, potassium ions will leave the cell. The voltage briefly goes below the membrane threshold due to it rushing towards the resting potential of K^+ and this is known as the "undershoot". Another action potential cannot be elicited until the membrane voltage returns to its resting potential. This period of time between the undershoot and the next action potential is known as the *absolute refractory period*.

When the cell is at rest, its voltage sits approximately between -70mV and -65mV, which is close to the equilibrium potential of the potassium ions inside the cell. When the membrane receives stimulation from an excitatory input, this causes the membrane voltage to have a brief depolarisation. If these stimulations cause a voltage increase above the "membrane threshold" of -55mV, the action potential is invoked and the cell depolarises rapidly towards the equilibrium potential for sodium ions, +62mV. This is due to the large "driving force" on sodium ions from the negatively charged cell membrane at rest. Hence, when the membrane threshold has been reached, the sodium channels open briefly allowing sodium ions to rush through and to further drive the cell potential positive. The overshoot comes from the potential rising above 0V towards the equilibrium potential of sodium (E_{Na}). Into a millisecond of the action potential, the sodium channels inactivate while the potassium channels remain open. This means that potassium can flow back into the cell and drive the potential back down. As the cell was positively charged previous to this, the potassium ions are now strongly drawn back into the cell due to a smaller concentration gradient inside the cell which causes the membrane potential to become negative again.

However, as there is now a higher proportion of potassium ions to sodium ions inside the cell, the voltage potential of the cell goes towards the equilibrium potential for potassium ions (E_K) at -80 mV. This remains like this until the potassium channels close again. The absolute refractory period is when the sodium channels become inactivated as a result of strong depolarisation of the cell, and they cannot reset to an active state until the membrane potential of the cell returns to a slightly less negative voltage towards the cell resting potential of -65mV.

What Hodgkin and Huxley did during their series of experiments of the giant axons seen in squids was to come up with a model which explained the underlying mechanisms of an action potential in this giant axon [19, 20, 21, 22].

It is worthy to note that in the case of the squid axon, there are only two voltage-dependent processes as opposed to that seen in mammals. Those two are the sodium and potassium conductances.

They found that the fundamental processes behind the action potential came from two main

conductances; the sodium conductance, G_{Na}, and the potassium conductance, G_K as well as a smaller contribution from the "leak" conductance, G_l, which doesn't depend on the membrane potential. This allows the total membrane current to be catergorised into its separate elements. The total membrane current, due to the sum of ionic currents and capacitive current, is then expressed as:

$$C_m \frac{dV_m}{dt} + I_{ion} = I_{ext} \tag{14}$$

C_m is the membrane capacitance, V_m is the intracellular potential (or membrane potential). I_{ion} is the sum of the ionic currents flowing across the membrane, and I_{ext} relates to an externally applied current.

6.1 Electrical Equivalent circuit for Squid Axon patch

The Hodgkin-Huxley model takes the squid axon nerve and models it as two passive components, the capacitance C_m and leak conductance G_l (flowing out of the cell), and two active voltage-dependent components, G_{Na} and G_K as seen in Fig.12.

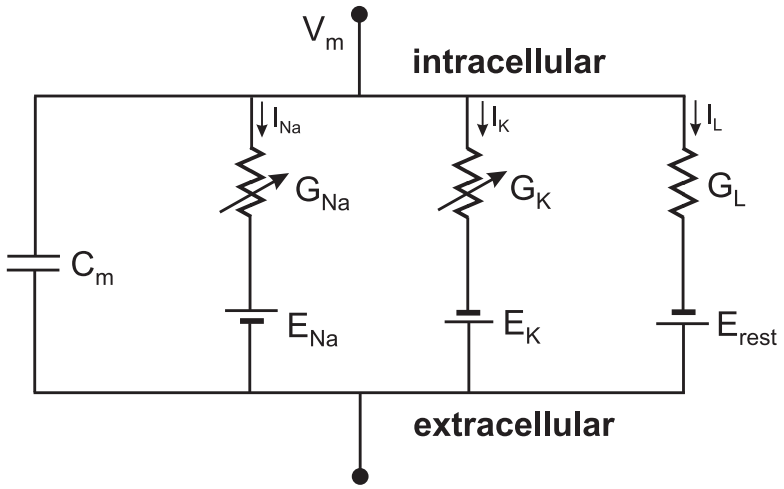

Figure 12: Circuit equivalent diagram of cell membrane, based on the work from Hodgkin and Huxley. The capacitance, C_m represents the phospholipid bilayer. G_K, G_{Na} and G_{leak} are the associated potassium, sodium and leak conductances carried by the ions travelling in and out of the neuronal membrane.

The total ionic current which flows is the sum of the sodium, potassium and leak current:

$$I_{ion} = I_{Na} + I_K + I_{leak} \tag{15}$$

This can be rewritten in terms of Ohm's Law:

$$I_{ion} = G_{Na}(V_m - E_{Na}) + G_K(V_m - E_K) + G_L(V_m - E_L) \tag{16}$$

As we can see, each ionic current has an associated conductance G_K and equilibrium potential, E_K. The expression $I_k = G_k(V_m - E_k)$ comes from the assumption that the ionic current is proportional to the sum of the conductance and driving force (membrane potential).

The equilibrium potential for each ion is calculated using the Nernst equation (see Appendix B).

At the time of Hodgkin and Huxley's experiments, there was no definitive evidence of what exact membrane channels existed and they instead came up with voltage-dependent "gating particles" to describe the dynamics of the conductances. These gating particles described the activation and inactivation of the channels. These particles can only be in one of two states, open or closed, and this being dependent on time and membrane voltage. When these gates for a particular ion are *all* "permissive" at the one time, ions can pass through the channel. The channel is then referred to as being open. If any of the gates are in a "non-permissive" state, then the gate remains closed.

6.1.1 The Potassium Current, I_K

Taken from Hodgkin and Huxley's 1952d paper [22], the modelled potassium current, which has a higher ratio of ions *inside* the cell, is given by:

$$I_K = \bar{g}_K n^4 (V - E_K) \tag{17}$$

g_K is the maximal conductance and given in units of mS/cm^2, the potassium battery E_K is relative to the resting potential of the axon. n describes the state of the "activation particle" and is a dimensionless number between 0 and 1. As we have n^4, this means there are 4 n states we are

looking at. It can be thought of representing the probability of a gate being in a permissive state. If we presume that the probability of a gate opening (or being in the permissive state) is n, then the probability of the gate being non-permissive or closed is 1-n. A non-permissive state is when there is no current flowing through the conductance. All gates have to be permissive to allow the channel to open, therefore, if one of the gates are in a non-permissive state then the potassium channel remains closed.

Hodgkin and Huxley assume that there are only these two states of "permissive" and "non-permissive" for a single particle and that this development between the states can be described using a first-order kinetics model. This can be written as:

$$n \underset{\alpha_n}{\overset{\beta_n}{\rightleftharpoons}} 1 - n \tag{18}$$

Where α_n is a voltage-dependent rate constant, given in units of 1 per second. The rate constant specifies how many transitions occur between the closed and open states whereas β_n expresses the number of transitions from the open to the closed states again given in units of 1 per second. We can then write this relation as a first-order differential equation:

$$\frac{dn}{dt} = \alpha_n(V)(1-n) - \beta_n(V)n \tag{19}$$

These rate constants α_n and β_n can also be described in voltage-dependent terms:

$$\frac{dn}{dt} = \alpha_n(V)(1-n) - \beta_n(V)n \tag{20}$$

where τ_n =

$$\tau_n = \frac{1}{\alpha_n + \beta n} \tag{21}$$

and n_∞ =

$$n_\infty = \frac{\alpha_n}{\alpha_n + \beta_n} \tag{22}$$

These are described in terms of a voltage-dependent time constant $\tau_n(V)$ and steady-state value $n_\infty(V)$.

Hodgkin-Huxley calculated the approximate voltage dependencies of the rate constants for the potassium conductance. They found that the relationship between the conductance and membrane potential is exponential and that when looking at the steady-state potassium membrane conductance for under 20mV, the conductance increases at an exponential rate when varying the voltage V by 4.8mV. Looking at the voltage sensitivity for the sodium conductance reveals that it has an even higher sensitivity.

Hodgkin and Huxley found that saturation of the membrane conductance occurred at higher levels of depolarisation [19] and described this relationship through the voltage-dependent rate constants [22]:

$$\alpha_n(V) = \frac{10 - V}{100(e^{(10-V)/10} - 1)} \tag{23}$$

$$\beta_n(V) = 0.125e^{-V/80} \tag{24}$$

V is the membrane potential relative to the axon's resting potential (mV). Figure 13 shows the voltage-dependent time constants and steady-state values of the potassium activation variable.

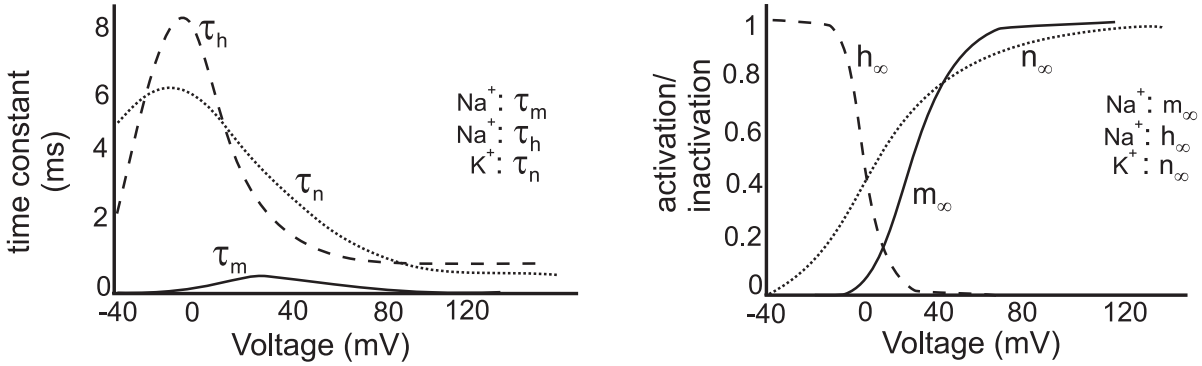

Figure 13: Activation and inactivation variables and time constants for each of the corresponding ion rate-variables.

Looking at these plots we can see that the time constant τ_n has a bell-shaped dependency for

each of the rate variables. However, n_∞ consistently increases with respect to the membrane potential. The plot of the relationship between the steady-state potassium conductance and membrane potential is exceptionally steep and this is seen in Eq.17 with the "fourth-power" relationship between G_k and n. A characteristic of many ionic conductances is that the effective conductance increases the more the cell membrane is depolarised.

Relating to the diagram of the sodium dynamics (Figure 13), we can see that there is a more complex evolution of the rate parameters.

6.1.2 The Sodium Current, I_{Na}

Using kinetics, Hodgkin and Huxley had to theorise that there was not just an activation particle, but also the existence of an inactivation particle for sodium. They describe the sodium current as [22]:

$$I_{Na} = \bar{g}_{Na} m^3 h (V - E_{Na}) \tag{25}$$

Where $g_{\bar{N}a}$ is the maximal sodium conductance when all the channels are open and was found by Hodgkin and Huxley to equal 120 mS/cm^2. The equilibrium, or resting potential, for sodium, E_{Na} = 115mV and is relative to the axon's resting potential. m and h are in dimensionless units with $0 \leq m, h \geq 1$. By convention, the sodium current is negative, that is, inward throughout the physiological voltage range (for $V < E_{Na}$). As we can see, the sodium conductance was modelled using three m gates and one n gate giving the four gating particles that make up the transition between the open and closed state for the ion channel. it should be noted that as well as m being the probability that the activating particle is "permissive", h is the probability that the "non-permissive" state is not in its inactivating state.

We now have two first-order differential equations which describe the rate constants:

$$\frac{dm}{dt} = \alpha_m(V)(1 - m) - \beta_m(V)m \tag{26}$$

and

$$\frac{dh}{dt} = \alpha_h(V)(1-h) - \beta_h(V)h \tag{27}$$

These voltage dependent rate constants were approximated once again by Hodgkin and Huxley as follows [22]:

$$\alpha_m(V) = \frac{25-V}{10(e^{(25-V)/10}-1)} \tag{28}$$

$$\beta_m(V) = 4e^{-V/18} \tag{29}$$

$$\alpha_h(V) = 0.07e^{-V/20} \tag{30}$$

$$\beta_h(V) = \frac{1}{e^{(30-V)/10}+1} \tag{31}$$

When referring back to Figure 13, we see that τ_m and τ_h are similar to that of τ_n. m_∞ is an increasing function of V which is what is expected, however, h_∞ decreases as the membrane depolarisation increases. This is a standard behaviour of the inactivation particle. If this inactivation particle were not to be included then the sodium conductance would remain at its maximum value in the presence of a depolarising voltage step.

6.2 Expressing The Complete HH Model

Before we can write the complete membrane model equation using the Hodgkin-Huxley expressions for the active components of the membrane, We also have to consider the passive and voltage-independent "leak" conductance. The leak conductance, G_l, is independent of the voltage and remains constant over time. Hodgkin and Huxley measured this conductance as G_l = 0.3mS/cm^2 and corresponds to a passive membrane resistance of R_m = 3333 Ω·cm^2. This passive element also has an associated membrane potential, however, Hodgkin and Huxley did not measure V_{rest} itself but

instead adjusted it to give a total membrane current of zero at the resting potential, V = 0.

V_{rest} was instead defined through the equation:

$$G_{Na}(0)E_{Na} + G_K(0)E_K = G_l V_{rest} = 0 \tag{32}$$

This was then calculated to be +10.613mV with membrane capacitance $C_m = 1\mu F/cm^2$. At the membrane resting potential, the effective membrane resistance due to the sum of the potassium, sodium, and leak conductances is equal to 857 $\Omega \cdot cm^2$. This is equivalent to a passive membrane time constant of roughly 0.85 ms.

We can now write an expression which describes all the currents flowing across the patch of axonal membrane:

$$C_m \frac{dV}{dt} = \bar{g}_{Na} m^3 h(E_{Na} - V) + \bar{g}_K n^4 (E_K - V) + g_l(V_{rest} - V) + I_{inj}(t) \tag{33}$$

We now have an idea of how action potentials are invoked from the observation of the Hodgkin-Huxley model of ion movement. As we are interested in modelling plasticity via biophysical parameters, it is therefore of great importance to now include a model of calcium dynamics, as we will find out in Section 7 the critical role these Ca^{2+} ions play in synaptic plasticity.

6.3 Calcium Dynamics

The movement of calcium ions during cell excitation and inhibition play a major role in the change in synaptic plasticity between neurons. They are important for signalling long term potentiation and long term depression. More clearly, the change in calcium concentration can signal either a strengthening or deterioration in connection between the pre- and postsynaptic terminals of a neuron.

We have discussed how Hodgkin and Huxley categorised the dynamics of sodium and potassium ions, and now we focus on how such dynamics can be represented for the Ca^{2+} ions. One such relevent publication by Desthexe et al catergorises many different types of calcium currents

[24], and their activation/inactivation particles are displayed in the same form as those categorised by Hodgkin and Huxley. The calcium current which has been implemented in our model is known as a "low-threshold calcium current", I_T, and its activation and inactivation variables are:

$$\begin{aligned} I_T &= \bar{g}_{Ca^{2+}} m^2 h (V - E_{Ca^{2+}}) \\ \dot{m} &= -\frac{1}{\tau_m(V)}[m - m_\infty(V)] \\ \dot{h} &= -\frac{1}{\tau_h(V)}[h - h_\infty(V)] \end{aligned}$$

$\bar{g}_{Ca^{2+}}$ = 1.75 mS/cm^2 and is the maximum conductance value of the calcium current, V is the cell membrane potential, $E_{Ca^{2+}}$ the reversal potential. m and h are the activation and inactivation variables and their functions and time constants are calculated from:

$$\begin{aligned} m_\infty(V) &= \frac{1}{1 + e^{-\frac{V+52}{7.4}}} \\ \tau_m(V) &= 0.44 + \frac{0.15}{e^{\frac{V+27}{10}} + e^{-\frac{V+102}{15}}} \\ h_\infty(V) &= \frac{1}{1 + e^{\frac{V+80}{5}}} \\ \tau_h(V) &= 22.7 + \frac{0.27}{e^{\frac{V+48}{4}} + e^{-\frac{V+407}{50}}} \end{aligned}$$

To use these parameters in our model, we then have to integrate them into the program environment we choose to use. In the GENESIS [8] source-code (the simulator we use to code our model), the change in calcium concentration is calculated from a single-pool exponential:

$$dCa^{2+}/dt = B \cdot I_{Ca^{2+}} - Ca^{2+}/\tau_{Ca^{2+}} \tag{34}$$

This models the low-threshold calcium current, $I_{Ca^{2+}}$, with parameters: $\bar{g}_{Ca^{2+}}$ = 1.75mS/Cm^2, decay-time $\tau_{Ca^{2+}}$ = 30ms, $[Ca^{2+}]_i$ = 2mM. $B = 1e12$ (1 / calcium charge ($C_{Ca^{2+}}$) multiplied by

the Faraday constant multiplied by the ion shell volume).

Ca^{2+} is the resulting concentration of the calcium ions and Ca^{2+}_{base} is the base-level concentration, giving Ca^{2+} = Ca^{2+}_{base} + Ca^{2+}. We can then show a plot of the low-threshold calcium current:

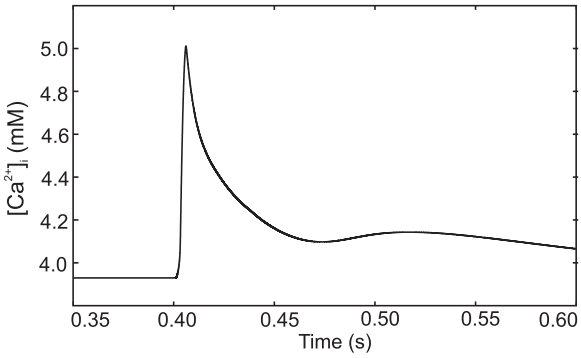

Figure 14: Calcium dynamics. The calcium model used was a single pool exponential of the form $dC/dt = B \cdot I_k - C/\tau$, modelling a low threshold calcium current, $I_{Ca^{2+}}$, with parameters: $\bar{G}_{Ca^{2+}}$ = 1.75mS/Cm^2, $\tau_{Ca^{2+}}$ = 30ms, $[Ca^{2+}]_i$ = 2mM, B = 1e12. Ca^{2+} is the resulting concentration of the Ca^{2+} ions and Ca_{base} the base-level concentration, giving $Ca^{2+} = Ca^{2+}_{base} + C$.

Implementing this in our model meant the task of writing a new calcium channel. The code for the channel, along with the other receptors and dynamics are in the Appendix (Section C). Now we have discussed synaptic inputs, simple spiking models and added ionic detail with the Hodgkin-Huxley model, we can move on to looking at synaptic plasticity.

7 Plasticity

Synaptic plasticity was first hypothesised as a mechanism for learning and memory by Canadian psychologist Donald Hebb in 1949 [25]. His proposal was that “neurons which fire together, wire together”. The idea was that the strength between two neurons would strengthen if the timing of firing from each was almost instantaneous, and that with repeated firing, these connections would continue to increase in weight. It was discovered later on by Bliss and Lømo in 1973 [26] that this was in fact true and the phenomenon was termed long term potentiation, or LTP. They found that by stimulating the pre- and postsynaptic terminals via high-frequency stimulation (HFS) resulted in a strengthening between the synapses during conditioning experiments. The opposite of this

behaviour is known as long-term depression (LTD), and occurs when the postsynaptic neuron is stimulated slightly before the pre-, resulting in a decline in synaptic strength.

7.1 Biophysical mechanisms of plasticity

In excitatory synapses, a neurotransmitter called glutamate is released from the presynaptic axon terminal and activates several types of postsynaptic receptors in the dendrite of the postsynaptic neuron. These postsynaptic glutamate-gated ion channels allow positively charged ions into the postsynaptic cell and these glutamate-dependent channels are known as AMPA and NMDA receptors and commonly found on many excitatory synapses.

The calcium ion elevation/reduction through the NMDA receptors are integral to the changes observed in plasticity, with elevations in Ca^{2+} influx causing long term potentiation, whereas a moderate rise in the influx tends to result in synaptic depression. This will be expanded upon in the synaptic potentiation and depression sections.

It has been previously mentioned that the NMDA receptor differs from the AMPA receptor in a few significant ways. Firstly, unlike the AMPA receptors, the NMDA-receptor conductance is dependent of the voltage. This is due to magnesium ions which sit in front of and *block* the receptor. This is known as the “Magnesium-block”. When the cell is at resting potential, any inward current going through the NMDA receptor is blocked. When the cell becomes depolarised, The Magnesium ions begin to move from the receptor and current is allowed to flow inwards. The other characteristic of the NMDA receptor is that it conducts calcium ions. The NMDA receptors can act in a similar nature to those of the behaviour described by Donald Hebb, showing that an increase in weighting between two neurons is facilitated by the influx of calcium ions into the postsynaptic NMDA receptor from a presynaptic input. Hence, it has been said that the magnitude of calcium ions which pass through the NMDAR can signify how much pre- and postsynaptic activation is present.

The NMDA receptor is also known to have another special property during plasticity changes, in that it is responsible for calculating any change in strength between two neurons, then signalling

this to the AMPA receptors, which update the weight strength. This is seen in figure 15 as a simple block diagram. The "signalling" behaviour is an important part of the model used and is fulfilled in our model by introducing a "learning rule" to dictate any changes in strength between connected neurons.

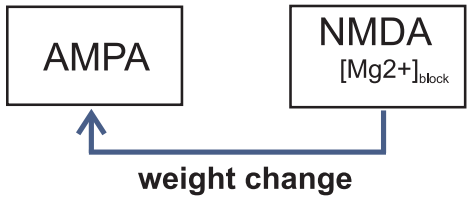

Figure 15: Block Diagram of how NMDA signals weight change between neurons. Na^+ ions enter the AMPA receptor allowing depolarisation of the cell membrane. This removes the Mg^{2+} block from the NMDA receptor and allows an influx of calcium through the receptor. The NMDA receptor acts as a "second messenger" calculating the weight change (implemented using a learning rule) and passing this to the AMPA receptor to update.

7.1.1 Mechanisms of synaptic potentiation

The simplest way to observe synaptic potentiation is to use high frequency stimulation (HFS) [26, 27] on the pre- and postsynaptic cell terminals to induce synaptic transmission from the presynapse. The presynaptic activation (an action potential generated from the presynaptic neuron) causes the release of glutamate, an excitatory amino acid known as a "neurotransmitter". This neurotransmitter acts on postsynaptic AMPA receptors by opening them and allowing the flow of sodium through to further depolarise the cell. This depolarisation allows the Mg^{2+} block to be lifted and then allowing the continuation of depolarisation by the influx of calcium into the receptors. This calcium influx is thought to enhance the synaptic effectiveness and thus associated with plasticity. Excitatory synaptic transmission in the hippocampus and the prefrontal cortex is thought to be governed by glutamate receptors. On the commencement of synaptic transmission, Na^+ ions which flow through AMPA receptors on the postsynptic neuron causes excitatory postsynaptic potentials. In addition to this, there is also the influx of calcium ions through NMDA receptors. The calcium flux occurs after glutamate binding to the NMDA receptor, and at the same time as the postsynaptic membrane is becoming depolarised. Depolarisation of the membrane then allows the

Mg^{2+} block to be lifted and calcium ions to enter trough the NMDA receptors. It can be said, therefore, that calcium ion entry through the NMDA receptors can be used to signal when the presynaptic and postsynaptic neurons are active at the same time. It has been shown by Lisman [27] that a rise in the concentration of calcium inside the postsynaptic cell, also known as the "intracellular calcium concentration" or $[Ca^{2+}]_i$, is linked with the induction of LTP. He states that significant influxes of Ca^{2+} through NMDA receptors cause an increase in the connection between two neurons, and also points out that this increase in synaptic weight is seen by the "enhanced" or increased magnitude in the synaptic current carried by Na^+ ions through the AMPA receptors. Thus, he states that LTP can be governed by a Hebbian-like rule, where constant stimulation of one cell onto another results in a prolonged episode of postsynaptic depolarisation. It should also be noted that while LTP can be invoked using high-frequency stimulation, during the event of spike-timing-dependent plasticity (STDP), discussed in the next section, LTP is only seen using low-frequency stimulation.

7.1.2 Mechanisms of synaptic depression

Classifying what mechansisms are exactly responsible has yet to be discovered, and this question is an integral part of the research. From what is known from physiologists is that it can be presumed that weak coincidence of spiking-events (action potentials) causes a decline in synaptic strength. In other words, if the postsynaptic neuron spikes before the pre- then a reduction in weight is observed [28, 29]. A weakened coincidence between two spikes (Action Potentials) could therefore cause a reduction in the NMDA-R activation causing a smaller influx of Ca^{2+}. Lisman also looked at long term depression, and proposed that if LTP is governed by Hebbian mechanisms, then LTD is mediated by "anti-Hebb" mechanisms [27]. This was thought to be the result of moderate increases in $[Ca^{2+}]$ through NMDA receptors which did not fully elicit action potentials in the postsynaptic cell.

Newer data on LTD from 2007 by Keiko Tanaka's lab looked at the crucial role Ca^{2+} played in synaptic depression [30]. They looked at the relationship between long term depression and the level of postsynaptic calcium ion concentration, to attempt to establish a relationship between them

and possible mechanisms. What was found was that the relationship between LTD and postsynaptic $[Ca^{2+}]_i$ could be described by a "leaky-integrator" function. Tanaka's lab found that they could induce long term depression by simply increasing the intracellular calcium concentration in the postsynaptic cell. It was the duration of elevated $[Ca^{2+}]_i$, however, which was the key factor in whether synaptic depression would happen or not. They reported that synaptic depression emerges from a mechanism that integrates the postsynaptic Ca^{2+} signals, and that the magnitude of LTD depended on the *level* of intracellular calcium concentration and duration of elevation, showing a leaky-integrator manner.

The relationship between LTD and $[Ca^{2+}]_i$ was also said to be sigmoidal in shape. Duration of $[Ca^{2+}]_i$ influenced the sensitivity of LTD. In simpler terms, there was a higher sensitivity to peak levels of intracellular calcium, and lower sensitivity to integrated $[Ca^{2+}]_i$ at longer time durations, described as a leaky integrator. Tanaka also showed that postsynaptic Ca^{2+} *alone* was enough in itself to induce synaptic depression, but, this is only true for $[Ca^{2+}]_i$ which pass a threshold level. In summary, their work on LTD found that its induction hinged on the rise in $[Ca^{2+}]_i$ above a certain threshold concentration. The level of $[Ca^{2+}]_i$ required for LTD was said to be comparatively low, but rather the timescale in which the $[Ca^{2+}]_i$ remains elevated is what governs if it will be seen. This study by Tanaka has played a crucial role in the research, so much so that in later sections when our model will be discussed, we refer to Tanaka's leaky-integrator expression for a mechanism of LTD.

The bi-directionality of synaptic weight discussed by Lisman and later elaborated on many other scientists [28, 31, 29], who looked at coincidental timing between pre- and postsynaptic timing between the spiking of coupled-neurons and its effect on synaptic weighting. This phenomenon was later termed "Spike-Timing-Dependent Plasticity".

7.2 Spike-Timing-Dependent Plasticity

Spike-Timing-Dependent Plasticity, or STDP, is a special phenomenon in plasticity dependent on the timing of pre-synaptic and postsynaptic action potentials, resulting in either an increase in

weight between the neurons, or decrease. The term itself was not fully established until a group of separate studies [28, 29, 31] all looked into how the millisecond timing of these action potentials could either weaken or strengthen the synaptic connection.

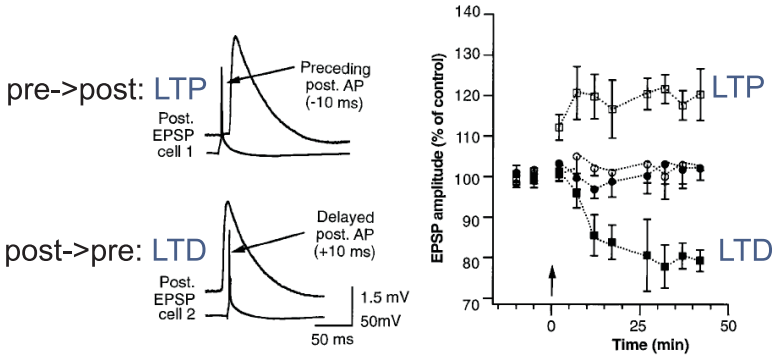

Figure 16: STDP curve taken from Markram et al. 1997 [28]. The left diagram shows the timing of the action potentials against the EPSPs. When the EPSP occurs before the postsynaptic action potential, a strengthening in plasticity is seen (LTP). When the timing protocol is reversed and the postsynaptic action potential is elicited before the EPSP, a decline in synaptic strength is witnessed (LTD).

The mechanisms behind LTP during spike-timing dependent plasticity are well-known to be a result of calcium influx into postsynaptic NMDA-Receptors. The mechanisms behind LTD are a little less clear. Magee and Johnstone and Henry Markram's research teams were both in close succession of each other when first looking into STDP, both specifically looking into the role of "Back Propagating Action Potentials" in the invoking of long term potentiation [31, 28]. Back-propagating action potentials are action potentials which travel from the postsynaptic soma back to the dendrites, and they are believed to play a major role in signalling changes in synaptic plasticity [31]. Magee states that these BPAPs provide a sufficient signal necessary in forming an association between the synaptic input and spiking action potential output. They suggest that due to the physical distance which separates the input from the output, a rapid feedback signal like the back-propagating action potential is sufficient to signal the association between the pre- and postsynaptic neuron, like a coincidence detection mechanism. Action potentials propagate quickly into the soma and dendrites and cause significant depolarisation to the cell membrane (EPSPs). Furthermore, this causes dramatic increases in the intracellular calcium concentration in the postsynaptic cell.

They noted that BPAPs which were inhibited by dendritic hyperpolarisation (when the mem-

brane potential is driven negative) resulted in the amount of action potentials invoked by correlated pre- and postsynaptic EPSPs becoming greatly reduced. This then meant the amount of postsynaptic action potentials propagating back to the dendrites was further reduced (or inhibited), causing a decrease in the pairing between neurons, also known as long term depression or LTD.

Markram's lab were also looking at the coincidence timing of postsynaptic action potentials and the EPSPs that they generated [28]. Their experimental results suggested that the coincidence between postsynaptic action potentials and EPSPs caused changes in the overall excitatory postsynaptic potentials generated. The amplitude of the EPSPs were significantly increased or decreased depending on the "precise-timing" of the postsynaptic action potentials with respect to the EPSPs. Like Magee, they found that BPAPs act as a modification signal in the strength between synaptic connections, dependent on the timing of the pre- and postsynaptic activity. Their main conclusion was that when postsynaptic action potentials occur in a time-window of 10ms before the EPSP, then the excitatory postsynaptic current (EPSC) magnitude was reduced (LTD). When the temporal order was reversed and the postsynaptic AP was elicited 10ms *after* the EPSP, then the EPSC magnitude was increased (LTP). This is seen in Fig.16.

The term "spike-timing-dependent plasticity" was first coined by Bi and Poo in their 1998 paper [29], and they furthered Magee and Markram's works by detailing the effect relative timings of pre- to postsynaptic spiking had on synaptic plasticity. They were also the first to use the more familiar style of STDP plot where both timings (postsynaptic spiking before pre- and vice-versa) are seen on the same plot (Fig. 17).

What's more is that further to showing the importance of spike-timing on plasticity, they claimed that both LTP and LTD were dependent on the activation of NMDA receptors, further establishing the notion that a moderate rise in $[Ca^{2+}]_i$ being responsible for synaptic depression and a transient increase in the intracellular calcium concentration resulting in potentiation. Potentiation was said to arise when repetitive low-frequency stimulation was applied to the presynaptic neuron. The EPSPs generated were capable of then invoking action potentials in the postsynaptic cell. When they measured the magnitude of the excitatory postsynaptic currents, their results

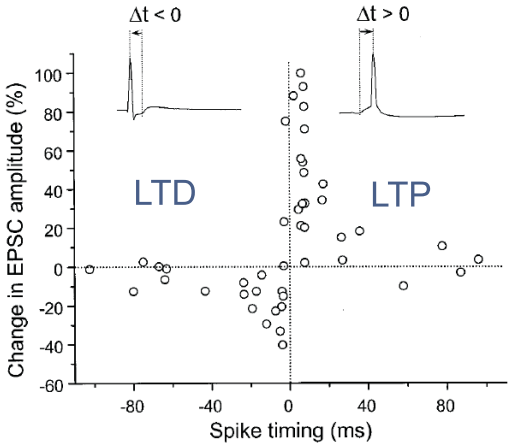

Figure 17: STDP curve taken from Bi and Poo 1998 [29].

showed that the repeated stimulation resulted in an increased synaptic plasticity between the two neurons. Their work on LTD was also important showing that repeated injections of current into the postsynaptic cell before the synaptic input resulted in a continual decline in EPSC amplitude, also known as LTD. This was termed negatively-correlated spiking.

In addition to showing that NMDAR's were crucial in LTP and LTD, Bi & Poo looked at the role of calcium channels in positive and negatively correlated spiking [29]. For the positive incidence, they said that the activation of voltage-gated calcium channels may occur collectively with NMDA receptors and that the influx of calcium through the channels work alongside the Ca^{2+} influx through NMDA receptors in initiating LTP [31, 29, 32]. In the negatively-correlated incidence, Bi & Poo found that a slower elevation of calcium ions through Ca^{2+} channels *before* synaptic activation (postsynaptic AP before presynaptic input) may be responsible for the initiation of synaptic depression.

It was therefore highly established that the influence of calcium influx during synaptic transmission was vital for both increased synaptic efficacy and reduced plasticity strength.

8 Computer Modelling of STDP

There are a wide variety of synaptic plasticity models used ranging from simple, abstract, spiking models through to more in-depth models which seek to accurately replicate biophysical mechanisms realistically. Of greatest relevance to the research, there have been two models by different laboratory groups. The first to be discussed, is the work from Harel Shouval and his research team. As mentioned in the previous section, NMDA receptor activity appears to be critical to the induction of synaptic potentiation and decline. Shouval, Bear and Cooper came up with a "unified model" of NMDA receptor-dependent STDP [33], where they quantified how much synaptic depression and potentiation could be seen, based on the amount of postsynaptic NMDA receptor activation during stimulation.

8.1 Shouval model of NMDA receptor-dependent STDP

Shouval's experimental work focused on looking beyond the initial discoveries [31, 28, 29] and concentrated on the role of Ca^{2+} influx through NMDA receptors, in an attempt to use a single "learning rule" which would dictate whether strengthening or depression between synapses would occur. Their protocol was to run these experiments under the same, although computer-modelled, conditions as those used by Markram et al. One idea that was fundamental in their model was that modest increases in postsynaptic Ca^{2+} through NMDA receptors triggers LTD, whereas transient increases in Ca^{2+} influx would result in LTP, as previously noted by Lisman, amongst others [27, 34, 35]. They draw from evidence [36, 37] that a moderate elevation in Ca^{2+} correlates with the induction of LTD, while larger, transient, elevations trigger the onset of LTP. Thus establishing the importance of Ca^{2+} in determining the sign and magnitude of synaptic plasticity.

In this paper, Shouval makes three key assumptions for his model to work. The first is that Ca^{2+} is the primary signal required for synaptic plasticity. The second is that the majority, or dominant source, of Ca^{2+} influx to the postsynaptic neuron goes through NMDA receptors. Lastly, is the role of back-propagating action potentials. In Shouval's model, those BPAPs contributing to STDP

have a slow, “after-depolarising” tail component to them.

For his first assumption (Ca^{2+} being the primary signal required), he sets thresholds for which calcium levels determine if LTP or LTD will occur. If the intracellular Ca^{2+} concentration goes above the first threshold, Θ_d, then LTD will occur. If the intracellular concentration surpasses the top threshold, Θ_p, then long term potentiation should be expected. When looking at the pairing of postsynaptic activity with pre- (referred to as post-pre stimulation), and vice-versa (pre-post), NMDA receptors are said to be the largest source of calcium influx to the postsynaptic neuron. Shouval goes on to say that the *change* in postsynaptic calcium concentration is mediated by the NMDA receptor activity, and the activation of the NMDAR’s dictate how much or little Ca^{2+} influx is seen in the postsynaptic neuron.

For his experiments, LTP is seen when the pre-post stimulation protocol produces a large elevation in postsynaptic $[Ca^{2+}]_i$, which should go above the higher concentration threshold, Θ_p. It makes sense that in his model, for LTD to be seen, we have a reversal of these requirements. That is, during post-pre stimulation, the $[Ca^{2+}]_i$ must only increase very modestly, so as to only go above the bottom threshold for Ca^{2+} influx (Θ_d) for long-term depression to be seen. Linking in Shouval’s third assumption of BPAPs having a slow after-depolarising tail, he states that the influence of the BPAP to the sign of the plasticity plays a role on Ca^{2+} influx through the NMDA receptor.

An interesting finding from Shouval’s work was that of pre-post LTD seen, showing a more symmetrical STDP curve in comparison to that seen in Bi & Poo’s 1998 paper [29]. This pre-post LTD was seen when the timing-window for stimulation was extended beyond the standard +20ms time-scale. Shouval claims that this pre-post LTD may be due to the number of NMDA receptors in an “open-state” continuously reducing after initial binding of glutamate to NMDARs. He says that this may be responsible, in conjunction with the level of Ca^{2+} required for LTD sitting at an intermediate value. This value has been suggested as one between a concentration that causes no change in plasticity, and one which would go on to produce LTP (above Θ_p).

The phenomenon of pre-post LTD has still to be widely recognised or rejected, and Shouval states that if there are further experiments which go on to falsify his findings, then his calcium

hypothesis should be adapted.

8.1.1 Refinement of Shouval Model

In 2005, Shouval went on to look at stochastic properties of NMDA receptor activity and calcium influx [38], to attempt to provide an explanation for the pre-post LTD witnessed in his previous experiments. He states that their original prediction of pre-post LTD had not yet been fulfilled in experimental conditions, with the exception of data found by Nishiyama's lab [39]. This has been put down to the lack of experimentation in the later regions of Δt beyond +20ms. This later paper is an elaboration by Shouval of the pre-post LTD and a refinement of the Ca^{2+} dynamics used in their model. Their model still uses lower and higher threshold bands (Θ_d and Θ_p), but now includes scenarios where the glutamate neurotransmitter fails to be released from the presynapse. Consequently this results in a failure to bind to the postsynaptic NMDAR, and thus, a failure in Ca^{2+} influx to the postsynaptic receptor.

The Shouval model is one of great significance and relevance to the research undertaken. Many models attempt to use a single "rule" to govern the bi-directionality of synaptic plasticity. The work carried out over the past two years seeks to refine and update a plasticity rule known as the ISO learning rule [40, 41, 42]. Different from Shouval, the ISO rule is based on a differential-Hebbian rule [43] that decides plasticity strength from the correlation of the presynaptic activity with the *change* in postsynaptic activity.

8.2 The ISO learning model

Unlike Shouval's model where the change in $[Ca^{2+}]_i$ represents the postsynaptic activity, the ISO learning rule (Isotropic Sequence Order learning) updates synaptic weight based on the correlation of presynaptic activity with the *derivative* of the postsynaptic activity. The 2004 paper from Saudargiene and Porr [44] puts forward a model of synaptic plasticity using key mechanisms to determine the calculation of weight-change. Their paper suggests the temporal change (or derivative) of the postsynaptic membrane potential correlated with conductance of the NMDA receptor.

Like Shouval, they address that back-propagating action potentials play a role in STDP [45], however, this is strictly limited to the shaping of the curve. That is, fast decaying BP spikes are shown to produce a typical asymmetric STDP curve, whereas slow decaying BPAPs result in symmetrical Hebbian learning curves. The main aim of the paper was to provide an analytical solution of spike-timing dependent plasticity based on the biophysical properties of the neural membrane and NMDA receptor. Saudargiene et al address that higher levels of calcium influx lead to a potentiation in synaptic plasticity, and that synaptic depression occurs when there is a moderate rise in $[Ca^{2+}]_i$.

What distinguishes their model is that a differential term has been included to represent postsynaptic activity. It was put forward [46] that the *change* in Ca^{2+} concentration (through NMDARs) determines whether LTP or LTD is seen.

8.3 Why improve this model?

As stated, the research completed during the past two years seeks to further improve the ISO learning rule. It is not the rule as such which had to be re-thought. It was however, the components of the learning rule which was desired to be modified. More specifically, the biophysical properties modelled had to be refined with more detail. The task was to include NMDA receptor activity, calcium dynamics and also take into account the effect other ions have on the synaptic weight. Further to this, looking at how inhibitory neurons projecting onto an excitatory neuron affected the overall plasticity curve was of great interest, as this had previously not been investigated. Thus, we now proceed to look at how such a model should be constructed.

8.4 What type of model to use?

Many different approaches could have been taken when deciding what type of equivalent model would suit the research best. This is mainly due to the level of detail one can decide to begin the model from. Also, it is important to figure out whether one *has* to delve into levels of detail which may not be required. For example, two classical ways of modelling the neuron are known

as the cable theory model and compartmental modelling. Both allow a high level of detail to be modelled, both achieving this under different assumptions about the model, but also both being too high a level of detail required for the research. We build our model from the Leaky Integrate and Fire model described, with added Hodgkin-Huxley parameters. We then add more detail to the model with calcium dynamics, AMPA, NMDA and GABA-ergic receptors, to allow plasticity and inhibition to be modelled in a more realistic manner.

8.5 Merging theory with practice

Throughout the previous sections we have discussed the basic elements of the neuronal membrane, the ionic processes taking place, stages in synaptic transmission, and solid, stable models used to emulate them. We now go on to discuss the practical side of this research, that is, the implementation of our model. We go on to model two neurons, one a pyramidal neuron (excitatory), one an interneuron (inhibitory), and observe the synaptic plasticity during experiments like those carried out previously by others.

9 The Model

The software GENESIS [8] (GEneral NEural SImulation System) is an open-source software package which allows a variety of uses in computer modelling. It is described by its developers as a “General purpose simulation platform developed to support simulation of neural systems ranging from subcellular components and biochemical reactions to complex models of single neurons, simulations of large networks, and systems-level models”. It uses a hierarchical structure to allow modular programming similar to that of C++.

One of the appealing reasons to use GENESIS is that the user is not limited to the channels and synapses included in the standard version of the software. As the software is written in C, the user can create their own custom synapses/channels and receptors by recompiling the skeleton architecture of the software to include code written by the user. Realistic parameter values for the pyramidal

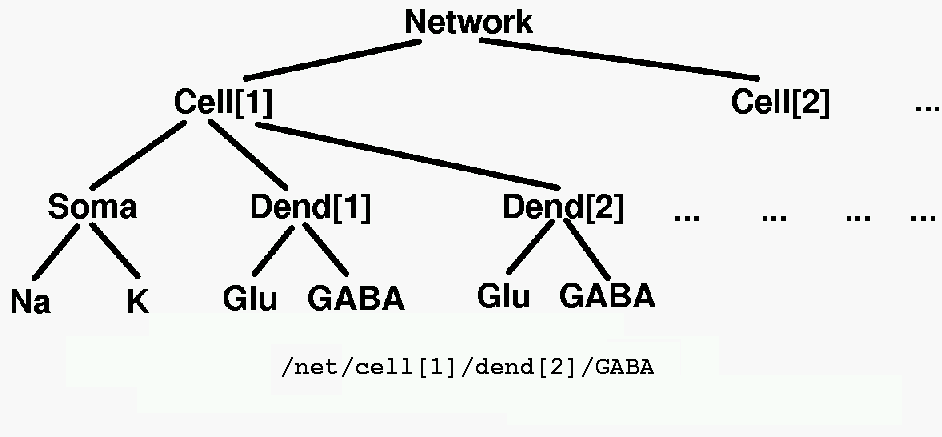

Figure 18: Hierarchical structure of GENESIS programming environment (taken from the Book of GENESIS [8].

cell conductance, membrane potential and NMDA/GABA conductances can be implemented into these receptors and channels by using values quoted from biology papers or from morphological data sites like neuromorpho.org[1].

As GENESIS uses compartmental modelling to represent a neuron, each segment of a cell (dendrites, soma, axon) can be constructed using separate compartments and then linked together using messages.

We use a simpler model of the neuron, using two compartments for each cell, one for the soma, and one for the axon.

9.1 Why use GENESIS?

We wish to use GENESIS to construct a reduced pyramidal cell model consisting of a soma and axon. The model was created using a custom-compiled version of the GENESIS-sim 2.3 modelling tool[8] and consists of a cortical pyramidal cell and attached GABAergic inhibitory interneuron (Fig. 19). To this model, we add the NMDA, AMPA and GABA receptors where appropriate, and implement Hodgkin-Huxley and modelled Ca^{2+} dynamics.

GENESIS allows linking of the two compartments using messages called “SPIKE” messages to

[1]http://neuromorpho.org/

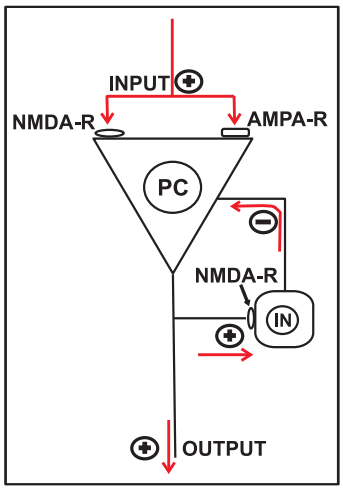

Figure 19: Graphical representation of model designed using the GENESIS-sim software. Here we can see the excitatory "input" which is the modelled presynaptic input into the pyramidal cell. The modelled action potential is simply a delta impulse function, Δt. Attached to the pyramidal cell are AMPA and NMDA receptors. A current injection into the pyramidal cell stimulates the neuron enough to generate the postsynaptic action potential. This travels from the pyramidal cell body and the axon activating the NMDA receptors on the GABAergic interneuron, allowing an influx of Ca^{2+} into the cell. If the excitation is strong enough the interneuron releases GABAergic neurotransmitters back to the pyramidal cell, inhibiting as it does so. Both the pyramidal cell and interneuron use the Hodgkin-Huxley model to implement ionic conductances realistically.

transmit information from the compartment and receive backwards. Once the cortical microcircuit has been constructed, the first objective was to study plasticity in the pyramidal neuron itself, then go on to add the interneuron and observe what effects this has on spike-timing-dependent plasticity. Further applications of the model involved looking at the microcircuit in reference to studies done in vivo and in vitro. Further to this, when reviewing results obtained from experimental data, we go on to link a study of hypofrontality, a condition which causes a decrease in cortical activity, in patients with impairment to receptors with our model which looks at plasticity and impairing the NMDARs to look at the effects of this.

9.2 Simulation Protocol

The spike-timing simulations are achieved by using two signals, one being the presynaptic input, and the other the postsynaptic stimulus. Through the difference in timing of invoked pre- and postsynaptic action potentials, we can look at the spike-timing-dependant plasticity of the small

network. This is done by observing the synaptic strength between the pre-and postsynaptic terminals, known as $\Delta\rho$. The presynaptic signal used is known as the "spiking input" (i.e. an excitatory input) and this input excites the postsynapse of the pyramidal cell. This is achieved in GENESIS by using a modelled action potential much like a delta impulse, δt. After a delay of 0.4s (chosen as the most suitable timing to apply the postsynaptic signal), the postsynaptic stimulation comes from a modelled current pulse injection into the soma. What results is a postsynaptic action potential. As these pre- and postsynaptic spikes are shifted through the simulation runtime from negative to positive timings (i.e. postsynaptic before presynaptic spikes towards pre-postsynaptic), the resulting synaptic weight-change $\Delta\rho$ is plotted as the familiar STDP curve.

Like the models discussed [44, 41, 33, 38], we have to specify a learning rule in our model which will calculate the change in synaptic plasticity as a result of the biophysical parameters present. In our model, we hope to use a learning rule which reflects processes undergone during in-vitro and in-vivo STDP experiments.

9.3 The Learning Rule

One of the main reasons behind using this model was to attempt to establish the mechanisms involved in plasticity by implementing them in a "learning rule". Previous to this model, Saudargiene et al [44] used a learning rule based on NMDA conductance correlated with the change in postsynaptic membrane voltage, which was later deemed to be unrealistic. What we wish to do is to update this learning rule with processes thought to be more realistic. This is done by separating the learning rule into two parts, one which calculates the weight change for pre-post stimulation, and the other for post-pre, all the while remaining as a single rule describing the plasticity changes.

It has been discussed in Section 7 that AMPA receptors play a role in updating the synaptic weight change which has been reliant on the NMDA receptor activity. Thus, in the simulation, the change in weight between synapses is calculated by the NMDA receptors and is then updated by the AMPA receptor. The calculated AMPA receptor weight, $\Delta\rho$, is updated through every step of the simulation:

$$\Delta\rho = LTP + LTD \tag{35}$$

where:

$$LTP = \mu \cdot NMDA_{act} \cdot \Theta([Ca^{2+}]'_i) \tag{36}$$

As it is seen, the mechanisms for LTP and LTP have been separated into two parts. For calculation of a positive increase in synaptic strength we have the correlation of the NMDA receptor activity $NMDA_{act}$ with the positive derivative of the intracellular calcium concentration $\Theta([Ca^{2+}]'_i$, which is then multiplied by the learning rate, μ. Θ is simply the Heaviside function which takes the positive part of the calcium concentration.

For LTD, we have essentially the same components to the equation, with the exception of the Ca^{2+} part:

$$LTD = \gamma \cdot NMDA_{act} \cdot \Theta(-[Ca^{2+}]'_{filt}) \tag{37}$$

Taking the negative derivative of filtered Ca^{2+} outflux, $\Theta(-[Ca^{2+}]'_{filt}$ is the implementation of the leaky-integrator filtering of calcium that was discussed in Section 7.1.2 as a proposed mechanism of LTD by Tanaka[30]. Again, $NMDA_{act}$ is the NMDA receptor activity, and γ is the respective learning rate.

To see how the rule is broken up into the separate elements which make up the intricate mechanisms undergone during LTP and LTD, we can refer to the block diagram shown in Fig. 20 and compare to learning rule above (Equation 35).

The elements of the learning rule have also been plotted on the same diagram as to give an idea of how their properties contribute to the weight-change when correlated (Fig.21). The first is the simple calcium concentration derivative plot, which is required for calculations of LTP. Directly below the positive calcium concentration is the filtered, negative derivative of the calcium concen-

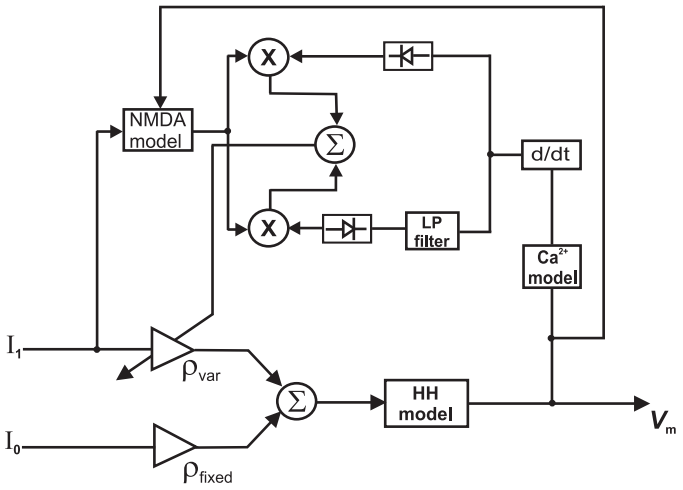

Figure 20: Block Diagram of STDP learning rule used. I_1 represents the variable spiking-event (current injection) timing, which can be altered to give either LTD or LTP depending on its occurrence before or after the fixed input, I_0. These two inputs are summated to give the timing difference between post and presynaptic spiking, T. In both parts of the learning rule there are HH ion channels and detailed calcium dynamics modelled. For both LTP and LTD, the derivative of the calcium concentration, $[Ca^{2+}]_i'$ is found. For LTP, the positive derivative of the $[Ca^{2+}]_i$ is taken. For LTD, the derivative is put through a lowpass leaky-integrator filter before taking the negative derivative of this. Both the positive and negative derivatives are dependent on NMDA-receptor activation which will affect the change in plasticity.

tration, which is used in the calculation of LTD. Finally, we see the NMDA receptor activation. It is well documented that the role of NMDA receptor activity is crucial in both the potentiation and fall in weight-strength between synapses.

We have now looked diagrammatically how each part of the learning rule is made up. Before looking at any results of STDP simulations, we finally have to look at how the leaky-integrator process written about by Tanaka [30] has been implemented in the GENESIS model.

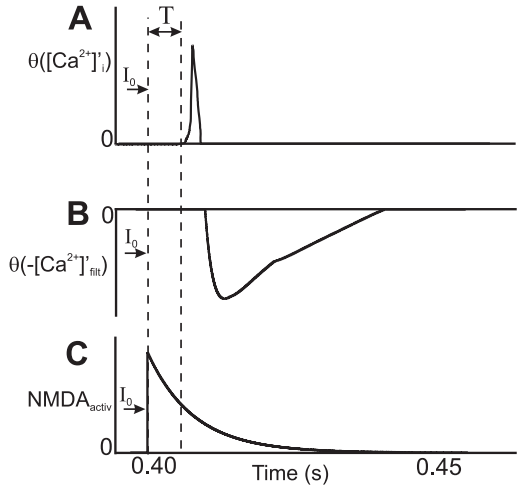

Figure 21: (a). Positive derivative of Ca^{2+} concentration, $[Ca^{2+}]'_i$, is used to model the positive part of the postsynaptic Ca^{2+} influx seen during LTP. (b). $[Ca^{2+}]'_{filt}$; the negative part of the filtered Ca^{2+} ($[Ca^{2+}]'_{filt}$ <0). We do this by filtering the calcium concentration using a leaky integrator model (Section 9.4), then taking the negative part of its derivative. (c). Activation of NMDA-R allows the influx of intracellular calcium to the postsynaptic receptor. Depending on how fully the receptor opens, the synaptic plasticity can either increase or decrease (LTP or LTD). I_0, the current injection, results in depolarisation of the cell which in turn enables the postsynaptic NMDA-Rs to open. T is the delay between I_0 and the NMDA-R opening, thus, any influx of Ca^{2+} into the receptor is delayed by T.

9.4 Modelling LTD - The Leaky-Integrator Filter

As mentioned, $[Ca^{2+}]'_{filt}$ is the negative part of the derivative of the intracellular calcium concentration ($[Ca^{2+}]'_{filt}$ <0). The study by Tanaka reported that a possible mechanism for LTD could be a slower outflux of calcium from the postsynaptic NMDA-Receptor [30] and was compared as a leaky-integrator filtering of the calcium. It was shown that having a slow and steady decay in $[Ca^{2+}]_i$ would result in LTD as opposed to LTP which occurs when there is a transient increase in $[Ca^{2+}]_i$. It was therefore decided this should be included in the learning rule.

Using a simple differential equation to give lowpass filtering of the calcium concentration, the derivative was calculated and then the negative part was used in the learning rule to express the LTD. The leaky integrator equation is in the form:

$$[Ca^{2+}]'_{filt} = [Ca^{2+}]'_{filt} + [Ca^{2+}]_i - ([Ca^{2+}]'_{filt} \cdot \tau) \tag{38}$$

Comparing the calcium concentration to the lowpass filtered concentration (Fig. 14), we can

see a slower decay in the concentration.

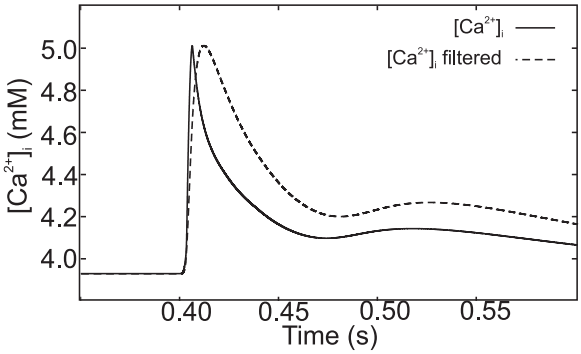

Figure 22: Comparison of Leaky integrator filtered Ca^{2+} against calcium concentration Filter constant τ = 0.8ms.

The code for the leaky integrator, along with the other code written can be found in Appendix C.

10 Results

Each simulation ran through 150,000 steps and STDP curves were generated by running single simulations repeatedly with a time shift 'T' between pre- and postsynaptic spiking events, starting from t = -0.10s to t = 0.10s and shifting in increments of 0.001s. The single simulation run-time is calculated by multiplying the number of simulation steps by $dt = 4e^{-6}$, giving a time of 0.6s. We now look at three separate STDP experiments. The first is looking at STDP in the pyramidal cell alone, the second looks at the changes in the STDP curve when a GABA-ergic interneuron is attached to the pyramidal cell. The third and final experiment is to look at what happens to STDP in the microcircuit when there is a reduction in NMDA receptor activity.

10.1 Pyramidal cell, no interneuron

In Fig.23, we have plotted three STDP curves, each using a different 'τ' value (τ = 0.8 ms, 0.05 ms and 5 ms) for the filtering of the Ca^{2+} outflux. On the Y-axis we have the change in weight, $\Delta\rho$, and this is plotted against the interspike interval T (X-axis), which is the timing between pre-

and postsynaptic spiking. The interspike interval is calculated by finding the values of the time of presynaptic spiking, t_{pre}, and subtracting this from the postsynaptic timing, t_{post}. It is observed that different filtering of the $[Ca^{2+}]_i$ produces three noticeably different STDP curves. While the LTP part remains consistently the same, we can clearly see there are three distinct alterations seen in the LTD part of the curve. By changing the decay constant 'τ' of the leaky integrator, we can directly affect the shape of the LTD seen which in turn changes the STDP plot shapes. Comparing Fig. 23(a) to Fig. 23(b), it can be observed that the time LTD is present during the negative time window is much longer. When the filter has a long decay time (Fig. 23(c)), there is a noticeable decrease in time as well as magnitude of LTD present. We can also make the general observation that the STDP curve Fig. 23(a) is strikingly similar to results seen in vitro [28, 31, 29].

10.2 Pyramidal cell with attached interneuron

As mentioned in Fig.19, the attached interneuron is a modelled GABAergic interneuron (known as a chandelier cell) with NMDA and GABA receptors, along with detailed HH channels [47].

However, instead of plotting three different curves using the different 'τ' values, we have chosen the 'τ' (0.8 ms) which allows for the most biologically accurate output. Again the weight change, $\Delta\rho$, is plotted against the interspike interval, T. When looking at the STDP curve of pyramidal cell with attached interneuron (solid lines) in comparison to without interneuron (dashed lines) in Fig. 24, it is interesting to observe the decline in magnitude and shape of LTD, while long-term potentiation remains the same. This is due to the dual nature of the GABAergic interneuron. In particular, the process of shunting inhibition from the $GABA_A$ receptors (which was discussed in Section 3.4) can result in some interesting behaviours affecting the pyramidal cell. Shunting inhibition, which as well as being inhibitory on the pyramidal cell, can lead to either depolarization or hyperpolarization of the postsynaptic cell depending on the GABAergic current. In the instance of our model, when hyperpolarization occurs, the pyramidal cell's membrane potential is driven negative towards the GABA reversal potential. This causes a dampening "shunting inhibition" on the pyramidal cell followed by depolarization causing an excitatory effect. Looking at the comparison

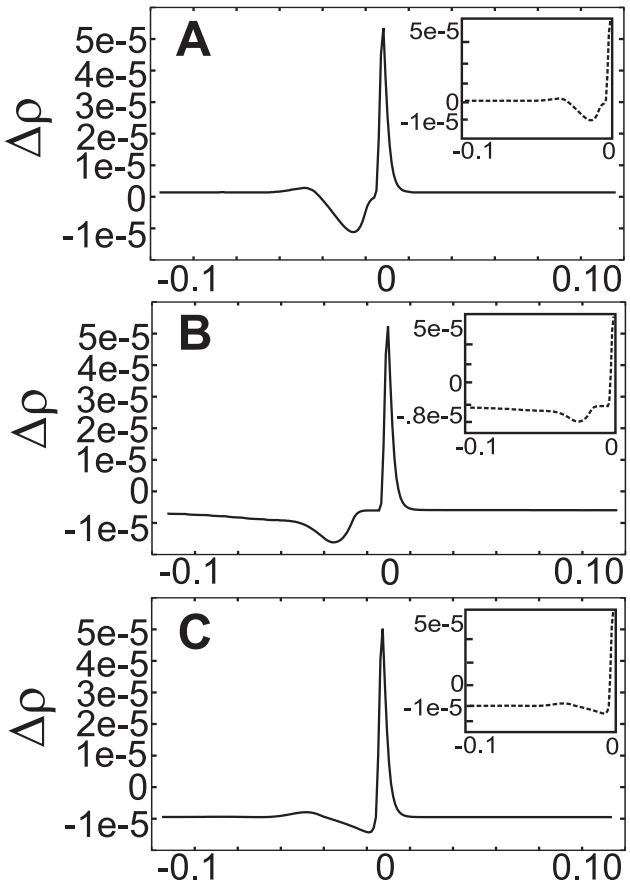

Figure 23: STDP using leaky-integrator modelled LTD. Insets in top right hand of each plot display LTD part of the STDP curve. (a). Leaky integrator time constant, τ = 0.8 ms. STDP curve looks like the expected asymmetrical weight-change curve. (b). Filtering of $[Ca^{2+}]_i$ with τ = 0.05 ms now gives a longer and larger LTD part to the STDP curve. (c). When the decay constant is set to τ = 5 ms, LTD significantly diminishes and lasts only for a short period (occurring just before $T < 0$s).

between with and without interneuron in Fig. 24, we can recognise that LTD is reduced when the interneuron is attached. It can be suggested that the inclusion of the interneuron during simulations causes excitation in the pyramidal cell. Even though the interneuron is inhibitory by nature, a small increase in conductance can lead to the membrane threshold of the pyramidal cell to be surpassed, and thus causing an excitatory effect on the cell resulting in less LTD being witnessed, as seen in Fig. 24 (dashed line).

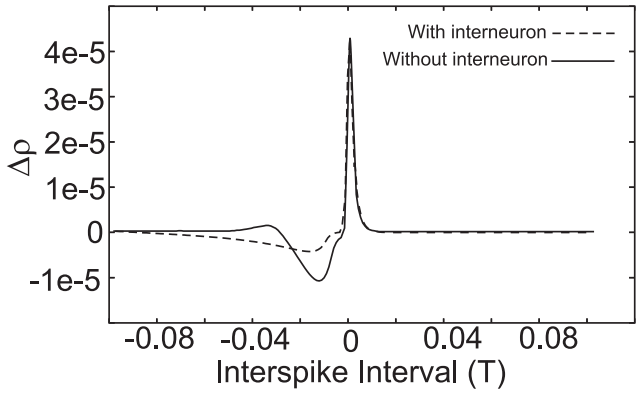

Figure 24: Comparison between STDP plots of pyramidal cell with (dashed line) and without (solid line) interneuron, both using τ = 0.8 ms. By comparing the STDP curve with attached interneuron to without interneuron (dashed line), a distinct decrease in magnitude in LTD is seen, which causes a noticeable shape change to the curve. We can then say that by adding the interneuron to the circuit, we are witnessing an increase in the excitatory activity in the pyramidal cell, which leads on to the reduction in synaptic depression (LTD). That is, during post-presynaptic spike-timings ($T < 0$), GABAergic conductance changes have an excitatory effect on the synaptic plasticity and cause LTD to be diminished.

10.3 Reducing the NMDA activation

NMDA receptors are responsible for the majority of calcium influx into a cell [48]. Therefore if there is an impairment to the NMDA receptors, we should observe two effects; a distinct decrease in magnitude of plasticity and a reduction in inhibition from the attached interneuron. From this, we can predict that a sizeable reduction in magnitude of the overall STDP curve should be seen as well as a complete change in shape to what was observed in Fig.24. When we study the effects the attached interneuron and NMDA receptor impairment has on the STDP curve, it is reasonable to conclude that reducing NMDA-R activity impairs the GABAergic inhibition on the pyramidal cell by decreasing the GABAergic conductance, $\bar{g}_{GABA}$. This disinhibition of the pyramidal cell's excitatory activity (due to the reduced GABA conductance $\bar{g}_{GABA}$) allows the pyramidal cell's membrane potential to increase, causing a potentiation in synapse strength during the negative timing window. Therefore, the amount of LTD seen in comparison to that seen in Fig. 25 is increased.

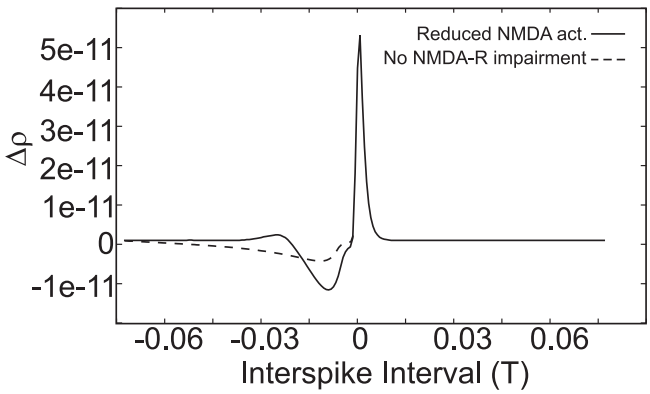

Figure 25: Reducing the NMDA receptor activity affects both the pyramidal cell and interneuron. Reduced NMDA activity will cause a decline in the influx of intracellular calcium into the pyramidal cell. Thus, any plasticity changes seen during LTP and LTD will be proportionally smaller and in ratio to the NMDA receptor activity. In addition to this, reduction in NMDA receptor activity will also affect the GABAergic interneuron. The reduction in NMDA-R activity means that the interneuron's ability to produce inhibitory GABAergic neurotransmitters will be drastically impaired. In turn, this causes the reduction in LTD previously seen in Fig.24 to be markedly reversed.

10.4 Conclusion

Through the research undertaken, the effects of adding an interneuron to a small cell-network has been shown to clearly modify the phenomenon of spike-timing-dependent plasticity. It has been determined that using a learning rule incorporating biophysical properties of the cell is sufficient to model mechanisms taking place during STDP. The background of cellular modelling along with comparative models within the field have been presented so as to demonstrate where this research picks up from. From using biophysical properties of the cell during synaptic activity, differences between STDP with and without the inhibitory interneuron have been presented, along with additional results showing that reduced NMDA activation can result in a reduction in the excitation of the interneuron, which thus goes on to diminish GABA release. It has been concluded that this model, as to date, has successfully been able to use a biophysically realistic learning rule to govern the plasticity changes seen during spike-timing-dependent plasticity. From these results it can be surmised that the addition of an inhibitory interneuron to a pyramidal cell will result in the reduction in Long-Term Depression observed during the STDP simulations, suggesting that the interneuron has an excitatory effect on the pyramidal cell. By reducing the NMDA-Receptor activity within the network, we were then given the opportunity to look at a topical hypothesis currently in the field of Neuroscience research. That is, the NMDA-Receptor impairment link currently being made to those who suffer from Schizophrenia. During the third simulation, we showed that by reducing NMDA-Receptor activation (Fig. 25), the previously seen excitatory effects of the interneuron (as seen in Fig. 24) had been reversed and were similar to that of when no interneuron was attached (Figures 23,24). It can be concluded that an impairment in NMDA-Receptor activity results in a decrease in the excitation of the interneuron, which in turn leads on to the reduced GABAergic activity in the cell. Thus, the overall effect that the interneuron has on the network is impaired.

The results of these three STDP experiments have been thoroughly considered and compared to relevant in vitro/vivo data in the field [28, 29, 31, 49, 50, 51]. It is also important to discuss what impact these results have, what improvements could and should be made to the model, and most crucially, how these results can be used.

11 Discussion

We have shown that it is possible to model Ca^{2+} dependent LTD realistically during STDP simulations. Rather than have set Ca^{2+} concentration thresholds which determine whether LTP or LTD should take place, as is the case with Shouval's model [33], our approach determines LTP and LTD by the *rate of change* in calcium influx/outflux. By using our biophysically realistic learning rule, which applies differential Hebbian learning to scale the LTP/LTD parts separately, we have eliminated the positive-timing LTD that was seen by Shouval and Aihara [12, 33, 38], but *not* seen during in-vitro experiments [28, 31, 29]. Our model eliminates positive-timing LTD through the slow release of calcium, meaning the IPSPs generated during the LTP-window will not be strong enough to cause depolarisation of the postsynaptic membrane, thus eliminating the decline in synaptic strength.

Comparing our new learning rule to those such as the ISO learning rule [44, 42, 41, 40], the greatest noticeable difference between the two is the inclusion of Hodgkin-Huxley parameters and realistic calcium dynamics. Also, it can be noted that our new learning rule has been split into two separate terms which describe the pre- and postsynaptic mechanisms of LTP and LTD rather than one term describing all. This allows for a greater precision in the modelling of the cellular processes undergone during spike-timing plasticity.

In our implementation of the leaky integrator filtering of Ca^{2+}, we have shown that it is possible to model the relationship between Ca^{2+} dynamics and LTD, as stated by Tanaka [30]. However, the LTD seen may actually be caused by mechanisms opposing the data found by Tanaka. New research [52, 53] has shown that the weakening of synapse strength translated as LTD could in fact be caused by a retrograde transmitter moving backwards into the presynaptic neuron through an NMDA receptor on the presynapse. This retrograde transmitter passing through the presynaptic NMDARs is then believed to cause the weakening of the synaptic strength. This finding allows for further research to be carried out to investigate this claim more thoroughly.

11.1 Applications

We know that hypofrontality is a condition seen in patients with schizophrenia, and with our model we have replicated this decrease in cortical activity. By reducing the NMDA receptor activity, we are actively causing an increase in the LTD seen, shifting the ratio of LTD/LTP towards that of LTD. Observing our results when NMDA-R activation is reduced (Fig. 25), the inhibition that was seen when attaching an interneuron (Fig. 10) has now been reversed and causes an *increase* in LTD. Using this information along with studying the effects of NMDA-R impairment on the inhibitory interneuron, we can note the obvious changes in the balance between LTP and LTD. It was seen by Tegner et al and Song et al that the ratio of LTD to LTP (α = LTD/LTP) is essential for stable learing to occur [54, 55]. In particular, a balanced firing rate requires a learning ratio slightly larger than unity.(α = LTD/LTP $>$1.00). We hypothesise that the NMDA-R reduction causes a shift in the balance between LTD/LTP causing the alpha value, α, to become significantly larger than unity gain. We propose the larger ratio of LTD to LTP acts as a catalyst in causing hypofrontality. Expanding our model to a larger network would allow observations in the change in ratio of depression to potentiation, α = LTD/LTP, towards LTD in patients with hypofrontality.

Thus, a possible application for this model would be to develop the microcircuit into a larger network of neurons and observe working memory when there is NMDA receptor impairment. This type of model would be of interest to those who are working in the research field of schizophrenia [50, 51]. A further improvement on the model is to look at which NMDA-Receptor subtypes are actually responsible for long-term depression. It has recently been found [52] that LTD might actually be a result from activation of presynaptic NMDA receptors. Further investigation has to be done before applying this to the model.

There could also be further investigations carried out to look at what effect the interneuron has on plasticity changes, focusing on the GABAergic strength projecting onto the neuron, as well as the effects it has on spike-timing. It would also be beneficial to look at more complex stimuli to the circuit, and observe how plasticity is altered during bursts of spikes, which would further add to the biophysical realism of the model.

References

[1] K.D. Miller. *Receptive Fields and Maps in the Visual Cortex: Models of Ocular Dominance and Orientation Columns*. Springer Verlag, NY, 1996a.

[2] E. Erwin and K.D. Miller. *Modelling Joint Development of Ocular Dominance and Orientation Maps in Primary Visual Cortex*. Academic Press, 1996.

[3] W. Rall. Membrane Time Constant of Motoneurons. *Science*, 126:454, 1957.

[4] W. Rall. Branching dendritic trees and motoneuron membrane resistivity. *Exp Neurol*, 1:491–527, 1959.

[5] W. Rall. Time constants and electrotonic length of membrane cylinders and neurons, 1969.

[6] W. Rall. Core conductor theory and cable properties of neurons. in: Handbook of Physiology. The Nervous System. Cellular Biology of Neurons. *Am Physiol Soc*, 1:39–97, 1977.

[7] H. Markram. The blue brain project. *Nature Reviews Neuroscience*, 7:153–150, February 2006.

[8] J.M. Bower and D. Beeman. *The Book of GENESIS: Exploring Realistic Neural Models with the GEneral NEural SImulation System (2nd Ed.)*. Springer-Verlag, New York, 1998.

[9] C. Koch (Ed). *Biophysics of Computation: Information Processing in Single Neurons*. Oxford University Press, New York USA, 1998.

[10] T.M. Jessell and E.R. Kandel. Synaptic transmission: A bidirectional and self-modifiable form of cell-cell communication. *Neuron*, 10:(Suppl.) 1–30, 1993.

[11] W. Rall. Distinguishing theoretical synaptic potentials computed for different soma-dendritic distributions of synaptic input. *J. Neurophysiol.*, 30:1138–1168, 1967.

[12] T. Aihara, Y. Yamazaki Y. Abiru, Y. Fukushima H. Watanabe, and M. Tsukada. The relation between spike-timing dependent plasticity and Ca^{2+} dynamics in the hippocampal CA1 network. *Neuroscience*, 145:80–87, 2007.

[13] E. O'Mann and O. Paulsen. Keeping Inhibition Timely. *Neuron*, 49(1):8–9, 2006.

[14] T.J. Lewis R. Jolivet and W. Gerstner. Generalized Integrate-and-Fire Models of Neuronal Activity Approximate Spike Trains of a Detailed Model to a High Degree of Accuracy. *J. Neurophysiol*, 92:959–976, 2004.

[15] R.B. Stein. A theoretical analysis of neuronal variability. *J. Biophys.*, 5:173–194, 1965.

[16] B. Knight. Dynamics of encoding in a population of neurons. *J. Gen. Physiol.*, 59:734–766, 1972a.

[17] L. Lapicque. Recherches quantitatifs sur l'excitation electrique des nerfs traiteé comme une polarisation. *J. Physiol. Paris*, 9:620–635, 1907.

[18] L. Lapicque. *L'excitabilité en fonction du temps*. Presses Universitaires de France: Paris, France, 1926.

[19] A. L. Hodgkin and A. F Huxley. Currents carried by sodium and potassium ions through the membrane of the giant axon of *loligo*. *J. Physiol.*, 116:449–472, 1952a.

[20] A. L. Hodgkin and A. F Huxley. The components of membrane conductance in the giant axon of *loligo*. *J. Physiol.*, 116:473–496, 1952b.

[21] A. L. Hodgkin and A. F Huxley. The dual effect of membrane potential on sodium conductance in the giant axon of *loligo*. *J. Physiol.*, 116:497–506, 1952c.

[22] A. L. Hodgkin and A. F Huxley. A quantitive description of membrane current and its application to conduction and excitation in nerve. *J. Physiol.*, 117:500–544, 1952d.

[23] W. Rall. *Theoretical significance of dendritic trees for neuronal input-output relations.* Stanford University Press, Stanford, CA pp. 73-97, 1964.

[24] A. Destexhe, D. Contreras, T. J. Sejnowski, and M. Steriade. A Model of Soindle Rhythmicity in the Isolated Thalamic Reticular Nucleus. *Journal of Neurophysiology*, 2:803–818, 1994.

[25] D. O. Hebb. *The organization of behavior: A neuropyschological theory*. Wiley-Interscience, New York, 1949.

[26] T. V. Bliss and T. Lømo. Long-lasting potentiation of synaptic transmission in the dentate area of the anaesthetized rabbit following stimulation of the perforant path. *J. Physiol.*, 232:331–356, 1973.

[27] J. Lisman. A mechanism for the Hebb and the anti-Hebb processes underlying learning and memory. *Proc. Natl. Acad. Sci. USA*, 86:9574–9578, December 1989.

[28] H. Markram, J. Lübke, M. Frotscher, and B. Sakman. Regulation of synaptic efficacy by coincidence of postsynaptic APs and EPSPs. *Science*, 275:213–215, 1997.

[29] Guo-qiang Bi and Mu-ming Poo. Synaptic modifications in cultured hippocampal neurons: Dependence on spike timing, synaptic strengh, and postsynaptic cell type. *J. Neurosci.*, 18(24):10464–10472, 1998.

[30] K. Tanaka, L. Khiroug, F. Santamaria, T. Doi, H. Ogasawara, G. C. R. Ellis-Davies, M. Kawato, and G. J. Augustine. Ca^{2+} requirements for cerebellar long-term synaptic depression: Role for a postsynaptic leaky integrator. *Neuron*, 54:787–800, June 2007.

[31] J. C. Magee and D. Johnston. A synaptically controlled, associative signal for Hebbian plasticity in hippocampal neurons. *Science*, 275:209–213, 1997.

[32] A. Konnerth J. Eilers, G.J. Augustine. Subthreshold synaptic Ca^{2+} signalling in fine dendrites and spines of cerebellar Purkinje neurons. *Nature*, 373:155–158, 1995.

[33] M. F. Bear H. Z. Shouval and L. N. Cooper. A unified model of NMDA receptor-dependent bidirectional synaptic plasticity. *PNAS*, 99(16):10831–10836, August 2002.

[34] F.F. Ebner M. F. Bear, L.N. Cooper. A physiiological basis for theory of synapse modification. *Science*, 237:42–48, 1987.

[35] A. Artola and W. Singer. Long-term depression of excitatory synaptic transmission and its relationship to long-term potentiation. *Trends Neurosci.*, 16:480–487, 1993.

[36] A.C. Greenwood R.J. Cormier and J.A. Connor. Bidirectional synaptic plasticity correlated with the magnitude of dendritic calcium transients above a certain threshold. *J. Neurophysiol.*, 85:399–406, 2001.

[37] M.W. Brown K. Cho, J.P. Aggleton and Z.I. Bashir. An experimental test of the role of postsynaptic calcium levels in determining synaptic strength using perihinal cortex of rat. *J. Physiol*, 532:459–466, 2001.

[38] G. Kalantzis H. Z. Shouval. Stochastic Properties of Synaptic Transmission Affect the Shape of Spike Time-Dependent Plasticity Curves. *J. Neurophysiol.*, 93:1069–1073, 2005.

[39] M. Nishiyama, M.M. Poo K. Hong, K. Mikoshiba, and K. Kato. Calcium stores regulate the polarity and input specificity of synaptic modification. *Nature*, 408:584–588, 2000.

[40] B. Porr and F. Wörgötter. Isotropic sequence order learning using a novel linear algorithm in a closed loop behavioural system. *Biosystems*, 67(1–3):195–202, 2002.

[41] B. Porr and F. Wörgötter. Isotropic Sequence Order learning. *Neural Comp.*, 15:831–864, 2003.

[42] B. Porr and F. Wörgötter. Learning with “relevance”: Using a third factor to stabilise hebbian learning. *Neural Computation*, 19:2694–2719, 2007.

[43] P.D. Roberts. Computational Consequences of Temporally Asymmetric Learning Rules: I. Differential Hebbian Learning. *J. Comp. Neuroscience*, 7:235–246, 1999.

[44] A. Saudargiene, B. Porr, and F. Wörgötter. How the shape of pre- and postsynaptic signals can influence STDP: A biophysical model. *Neural Comp.*, 16:595–626, 2004.

[45] D.J. Linden. The Return of the Spike: Postsynaptic Action Potentials and the Induction of LTP and LTD. *Neuron*, 22(4):661–666, 1999.

[46] G. Q. Bi. Spatiotemporal specificity of synaptic plasticity: cellular rules and mechanisms. *Biol. Cybern.*, 87:319–332, 2002.

[47] A.L.Hodgkin and A.F.Huxley. A quantitative description of membrane current and its application to conduction and excitation in nerve. *J.Physiol*, 17(4):500–544, 1952.

[48] T. G. Oerthner B. L Sabatini and K. Svoboda. The life cycle of Ca^{2+} ions in dendritic spines. *Neuron*, 33:439–452, 2002.

[49] J. Vaisanen, M. Lakso A. Linden, U. Heinemann G. Wong, and E. Castren. Excitatory actions of NMDA receptor antagonists in rat entorhinal cortex and cultured entorhinal cortical neurons. *Neuropsychopharmacology*, 21(1):137–146, 1999.

[50] B. J. Morris, S. M. Cochran, and J. A. Pratt. PCP: from pharmacology to modelling schizophrenia. *Current opinion in Pharmacology*, 5, 2005.

[51] D. Rujescu, A.M. Hartmann A. Bender, M. Keck, H. Raeder F. Ohl, J. Genius I. Giegling, H.J. Moller R.W. McCarley, and H. Grunze. A pharmacological model for psychosis based on N-methyl-D-aspartate Receptor hypofunction: Molecular, cellular, function and behavioral abnormalities. *Biological Psychiatry*, 59(8):721–729, 2006.

[52] D.J. Brasier R. Corlew and B.D. Philpot. Presynaptic NMDA Receptors: Newly Appreciated Roles in Cortical Synaptic Function and Plasticity. *The Neuroscientist*, 14(6):609–625, 2008.

[53] J.C Madara and E.S. Levine. Presynaptic and Postsynaptic NMDA Receptors Mediate Distinct Effects of Brain-Derived Neurotrophic Factor on Synaptic Transmission. *J. Neurophysiol.*, 100:3175–3184, 2008.

[54] K. D. Miller S. Song and L.F. Abbott. Competitive hebbian learning through spike-timing-dependent synaptic plasticity. *Nature Neurosci*, 3:919–926, 2000.

[55] J. Tegnér and A. Kepecs. Why neuronal dynamics should control synaptic learning rules. in: Dietterich tg; becker s; ghahramani z (eds). *Adv Neural Inf Process Syst*, 14, 2002. MIT Press, Cambridge, MA.

A Conference Proceedings

A.1 CNS July 07

Shaping of STDP curve by interneuron and Ca^{2+} dynamics

Lynsey McCabe[1], Paolo Di Prodi[1], Bernd Porr[1], Florentin Wörgötter[2].

Spike-timing-dependent plasticity is a special form of Hebbian learning where the relative timing of post- and presynaptic activity determines the change in synaptic weight. Recent studies have shown that the shape of the postsynaptic potentials determine the shaping of the STDP curve.Consequently, interneurons change the shape of the postsynaptic potential, thus affecting the overall shaping of the STDP weight-change curve. The weight change rule used is split into two parts: LTP is modelled by NMDA activity multiplied by the derivative of the calcium concentration and LTD is modelled using Ca^{2+} only. The result of this is a STDP curve which depends of the Ca^{2+} dynamics, but is changed by the presence of the attached interneuron. Reduced NMDA activity in the model also presents an opportunity to model deficits seen by schizophrenia patients by observing the transformed plasticity plots. Reducing the NMDA activity not only reduces plasticity in the pyramidal cell, but also reduces the activity of the input NMDA receptor of the GABA-ergic interneuron. Therefor NMDA hypofunction has two effects; as well as scaling down LTP, there will also be a disinhibition of the interneuron, which will then cause an increase in LTD.

[1]Dept. of Electronics and Electrical Engineering, University of Glasgow, G12 8LT, Scotland.
[2]BCCN Göttingen, University of Göttingen, Bunsenstr.10 (at the MPI), D-37073 Göttingen, Germany.

A.2 CNS July 07

A working memory model with three factor learning

Paolo Di Prodi[1], Lynsey McCabe[1], Bernd Porr[1], FlorentinWörgötter[2].

Cortical models of working memory exhibit persistent activity which is needed in situations where temporal stimulus-stimulus or stimulus-rewards associations have to be learned. Individual neurons or small subgroups can be switched into persistent activity by a localized stimulus which we call CS whereas a global stimulus (US) is used to switch off the activity. To achieve this behaviour the network has to be fine tuned to prevent global oscillations or global silence. Here we present a working memory which fine-tunes its activity by itself and is learning stable persistent activity with the help of three factor Hebbian learning. The third factor serves here as a switch which enables learning only at certain moments. Here we switch on learning either at the moment of the CS or at the moment of the US. This leads to stable memory traces after a few trials. The third factor is motivated by the activity of dopaminergic neurons in the VTA which either fire at the moment of the CS or of the US.

[1]Dept. of Electronics and Electrical Engineering, University of Glasgow, G12 8LT, Scotland.
[2]BCCN Göttingen, University of Göttingen, Bunsenstr.10 (at the MPI), D-37073 Göttingen, Germany.

A.3 FENS July 08

Observing STDP of pyramidal cell and attached interneuron microcircuit using detailed Ca^{2+} dynamics

Lynsey McCabe[1], Paolo Di Prodi[1], Bernd Porr[1], Florentin Wörgötter[2].

Synaptic weight change sensitive to the relative timing of pre- and postsynaptic activity is known as spike-timing-dependent-plasticity, or STDP. We present a model where LTD is modelled by leaky integrator filtering of the change in Ca2+ concentration. The model consists of a pyramidal cell, attached interneuron (which performs feedback inhibition) and detailed Ca2+ dynamics. We show that attaching an interneuron to the pyramidal cell will greatly alter the overall asymmetry of the STDP curve, particularly observing a distinct reduction in LTD magnitude. In addition to this, we have shown that by reducing the NMDA-R activity, there is an overall reduction in the magnitude of the STDP weight-change curve. This is of particular interest in the research field of schizophrenia where patients are known to have NMDA-receptor impairment. From this study we have shown that the inhibitory interneuron greatly reduces LTD during STDP. The greater the inhibition from the interneuron, the less LTD is seen in the weight-change curve. By using our cortical microcircuit model, we show how NMDA hypofunction could be a possible mechanism of how the NMDA antagonist PCP causes cortical hypoactivity after a time lapse of a few days.

[1]Dept. of Electronics and Electrical Engineering, University of Glasgow, G12 8LT, Scotland.
[2]BCCN Göttingen, University of Göttingen, Bunsenstr.10 (at the MPI), D-37073 Göttingen, Germany.

A.4 SNG Aug 08

STDP in modelled cortical microcircuit using biophysically realistic learning rule

Lynsey McCabe[1], Paolo Di Prodi[1], Bernd Porr[1], Florentin Wörgötter[2].

Spike-Timing-Dependent Plasticity, or STDP, is a well-known phenomenon reliant on the specific timing between pre- and postsynaptic neural activity. We present a learning rule which uses postsynaptic NMDA processes correlated with calcium influx to calculate LTP. For LTD, the presynaptic NMDA activation is correlated with a retrograde transmitter. Our results successfully reproduce data taken from neurophysiological experiments. The model used is a cortical microcircuit and consists of a pyramidal cell, attached interneuron (which performs feedback inhibition) and detailed Ca2+ dynamics. By adding the interneuron to the pyramidal cell, we show that the effect of the GABAergic inhibition causes an altered symmetry of the weight-change curve as well as changing the time-window and shaping of LTD. We go on to show the influence NMDAR impairment has on the microcircuit and how this leads to a shift in t he ratio of LTD/LTP seen during STDP. Observing the strong influence the inhibitory interneuron along with NMDAR impairment has on the pyramidal cell, we theorise that these may play a possible role in hypofrontality seen in patients with schizophrenia.

[1]Dept. of Electronics and Electrical Engineering, University of Glasgow, G12 8LT, Scotland.
[2]BCCN Göttingen, University of Göttingen, Bunsenstr.10 (at the MPI), D-37073 Göttingen, Germany.

B The Nernst Equation

The Nernst equation is used to calculate the equilibrium voltage potential for an ion:

$$E_{ion} = 2.303\frac{RT}{zF}log_{10}\frac{[ion]_o}{[ion]_i} \tag{39}$$

E_{ion} is the ionic equilibrium potential, or "resting potential", R is the universal gas constant, T is absolute temperature (and proportional to E_{ion}), z is the charge of the ion, and is inversely proportional to E_{ion}. F is Faraday's constant and $[ion]_i$ and $[ion]_o$ are the ionic concentrations inside and outside the cell, respectively.

These are simplified when calculating at body temperature (37°C) as $\frac{RT}{F}$ becomes a constant:

$$E_k = 61.54mV \cdot log_{10}\frac{[K^+]_o}{[K^+]_i} \tag{40}$$

$$E_{Na} = 61.54mV \cdot log_{10}\frac{[Na^+]_o}{[Na^+]_i} \tag{41}$$

$$E_{Ca} = 30.77mV \cdot log_{10}\frac{[Ca^{2+}]_o}{[Ca^{2+}]_i} \tag{42}$$

Thus, when calculating the membrane resting potential at body temperature, we only need to know the intracellular and extracellular concentrations of the specific ions we are interested in.

C GENESIS Code

C.1 AMPA Receptor

```
/*==================================
Synaptic Channels
==================================*/

function make_AMPA_pyramid(path, name)

str path
str name

echo "creating AMPA pyramidal synapse in "{path}
pushe {path}
create ampalearn {name}
setfield {name} \
Ek {AMPArev} \ // reversal potential of the synapse
tau1 {tau1_ampa} \ // secs
tau2 {tau2_ampa} \ // secs
gmax {gextAMPA} // Siemens

pope
end



function make_AMPA_interneuron(path,name)

str path
str name

echo "creating AMPA interneuron synapse in "{path}
pushe {path}
```

```
create synchan {name}
setfield {name} \
Ek {AMPArev} \ // reversal potential of the synapse
tau1 {tau1_ampa} \ // secs
tau2 {tau2_ampa} \ // secs
gmax {gextI} // Siemens
pope
end
```

C.2 NMDA Receptor

```
/*=======================================
NMDA "learning" receptor
(allows implementation of plasticity rule)
=======================================*/

function make_NMDA_learning(path,name)

str path
str name

pushe {path}

create nmdalearn {name}
setfield {name}\
Ek {AMPArev} \ // same reversal potential as AMPA synapse
tau1 {tau1_nmda} \ // NMDA rise time (secs)
tau2 {tau2_nmda} \  // NMDA decay time secs
gmax {gextNMDA} // max NMDA conductance

create Mg_block {name}/Mg_block
setfield {name}/Mg_block \
CMg {CMg} \
```

```
KMg_A {1.0/eta} \
KMg_B {1.0/gamma}
addmsg {name} {name}/Mg_block CHANNEL Gk Ek
pope
end
```

C.3 GABA Synapse

```
/*-------------------------------------------------
"Generic" GABA synapse - gmax should be set later
according to type of neuron
-------------------------------------------------*/

function make_general_GABA(path,name)

str path
str name

pushe {path}

create synchan {name}
setfield {name}\
Ek {GABArev} \ // GABA reversal potential
tau1 {tau1_gaba} \ // secs
tau2 {tau2_gaba} \ // secs
gmax {gmaxGABA}

echo "GABAin created in "{path}
pope
end
```

C.4 Calcium Channel

```
// genesis script file - Ca_channel.g

float gcamax = -1e-12

// typical value for CA reversal potential is 120mV
float carev = -0.1 // Volts
float Vmin = -80e-3
float Vmax = 80e-3

// npoints resolution can be modified to suit...
int npoints = 8000

// Calcium concentration
float tauCA = 30e-3 // calcium depletion is slow
float Cain = 2 // intracellular calcium concentration... 2mM per litre
float B = 1e12
float CAbaseline = 0 // the baseline calcium concentration 0 mM
float shelltick = 1e-6



/*-----------------------------------------
Generated tabchannel to model low threshold
calcium current - Gbar is 1.75mS/Cmˆ2
-----------------------------------------*/



function m_inf_V(V)
float V
float minf=0;
float tempexp=0;
```

```
tempexp=-(V+52)/7.4
minf=1/(1+{exp {tempexp}})
return {minf}
end

function m_tau_V(V)
float V
float taum=0;
float tempexp1,tempexp2
tempexp1=(V+27)/10
tempexp2=-(V+102)/15
taum=0.44+(0.15/({exp {tempexp1}} + {exp {tempexp2}}))
return {taum}

end


// Fill the table with generated values
function fill_table_X(path,name)
str path
str name

pushe {path}

float Vstep={getfield {name} X_A->dx}
echo "Vstep is "{Vstep}
int index
int maxpts={getfield {name} X_A->xdivs}
echo "Points are  "{maxpts}
float V={Vmin}
for (index=0;index<={maxpts};index=index+1)
    float m_inf={m_inf_V {V}}
    float m_tau={m_tau_V {V}}
```

```
    setfield {name} X_A->table[{index}] {m_inf}
    setfield {name} X_B->table[{index}] {m_tau}
    V=V+Vstep

end//end for
pope
end

function h_inf_V(V)
float V
float hinf=0;
float tempexp=0;
tempexp=(V+80)/50
hinf=1/(1+{exp {tempexp}})
return {hinf}
end

function h_tau_V(V)
float V
float tauh=0;
float tempexp1,tempexp2
tempexp1=(V+48)/4
tempexp2=-(V+407)/50
tauh=22.7+(0.27/({exp {tempexp1}} + {exp {tempexp2}}))
return {tauh}

end


function fill_table_Y(path,name)
str path,name

pushe {path}
```

```
float Vstep={getfield {name} Y_A->dx}
echo "Vstep is "{Vstep}
int index
int maxpts={getfield {name} Y_A->xdivs}
echo "Points are  "{maxpts}
float V={Vmin}
for (index=0;index<={maxpts};index=index+1)
    float h_inf={h_inf_V {V}}
    float h_tau={h_tau_V {V}}
    setfield {name} Y_A->table[{index}] {h_inf}
    setfield {name} Y_B->table[{index}] {h_tau}
    V=V+Vstep

end//end for
pope
end

function gen_CA_conc(path,name)
str path,name
pushe {path}

echo "Generating CA conc in "{path}"with name "{name}
create Ca_concen {name}
setfield {name} B {B} tau {tauCA} Ca_base {CAbaseline} \
Ca {Cain} thick {shelltick}

end

function gen_CA_channel(path,name)
str path,name
pushe {path}
 create tabchannel {name}
```

```
echo "Generating tabchannel in "{path}" with name "{name}

 setfield {name} Ek {carev} Gbar {gcamax} Xpower 2 \
Ypower 1 Zpower 0

 call {name} TABCREATE X {npoints} {Vmin} {Vmax}
 call {name} TABCREATE Y {npoints} {Vmin} {Vmax}

 fill_table_X {path} {name}
 fill_table_Y {path} {name}

 tweaktau {name} X
 tweaktau {name} Y

echo "generating CaConc object in "{path}" with name CaConc"
gen_CA_conc {path} "CaConc"

addmsg {path}/{name} {path}/CaConc I_Ca Ik



pope
end
```

C.5 Leaky Integrator Filter

```
 if (channel->caconc_diff<0.0) channel->caconc_diff=0.0;

   channel->ltd_calc=(channel->ltd_calc)+((atof(caConcStr)) -
  \\  ((channel->ltd_calc)*(channel->tau_const)));
printf(" ltd calc is %f\n" , channel->ltd_calc);
channel->lowpassderiv= (channel->ltd_calc - channel->ltd_calc_prev);
channel->ltd_calc_prev= channel->ltd_calc;

printf(" low pass deriv %f\n" , channel->lowpassderiv);
       if ((channel->lowpassderiv)<0) {
          channel->lowpassderiv=((channel->lowpassderiv) * (channel->gainLTD));
        } else {
                channel->lowpassderiv=0.0;
        }
```

C.6 The Learning Rule

```
      /* channel->deltaNMDA calculates update of synapse weight */

        channel->deltaNMDA=(channel->mu * channel->X * channel->diff ) +
          \\((channel->gamma) * (channel->lowpassderiv) * channel->X);

/*  channel->mu and channel->gamma are learning rates, channel->X is NMDA
    activation, channel->diff is the positive derivative of calcium concentration
    and channel->lowpassderiv is the filtered negative derivative of the calcium
    concentration.*/
```

D Parameters

D.1 Ionic equilibrium potentials (SI Units)

- Pyramidal Cell E_{Na} = 0.055 V
- Pyramidal Cell E_K = -0.090 V
- Interneuron E_{Na} = 0.045 V
- Interneuron E_K = -0.10 V
- E_{leak} = -0.065 V

D.2 NMDA receptor

- Rise time τ_1 = 2 ms
- Decay time τ_1 = 10 ms
- $\bar{g}_{NMDA}$ = 15 nS

D.3 AMPA receptor

- Rise time τ_1 = 2 ns
- Decay time τ_1 = 2 ms
- $\bar{g}_{AMPA}$ = 1 nS

D.4 GABA receptor

- Rise time τ_1 = 10 ns
- Decay time τ_1 = 10 ms
- $\bar{g}_{GABA}$ = 25 nS //can be increased to implement shunting inhibition

D.5 Soma parameters for pyramidal cell

- Pyramidal Cell E_{rest} = -0.060 V
- Pyramidal Cell $\bar{g}_{leak}$ = 25 nS
- Pyramidal Cell R_m = $\frac{1}{\bar{g}_{leak}}$ Ω
- Pyramidal Cell C_m = 0.5 nF

D.6 Soma parameters for interneuron

- Interneuron E_{rest} = -0.070 V
- Interneuron $\bar{g}_{leak}$ = 20 nS
- Interneuron R_m = $\frac{1}{\bar{g}_{leak}}$ Ω
- Interneuron C_m = 0.2 nF